IEEE Access
Multidisciplinary | Rapid Review | Open Access Journal

Received February 3, 2020, accepted February 20, 2020, date of publication February 28, 2020, date of current version March 11, 2020.

Digital Object Identifier 10.1109/ACCESS.2020.2976672

Spatially Correlated Rayleigh Fading for Cell-Free Massive MIMO Systems

MENG ZHOU, YAO ZHANG, XU QIAO, AND LONGXIANG YANG
Wireless Communication Key Laboratory of Jiangsu Province, Nanjing University of Posts and Telecommunications, Nanjing 210003, China

Corresponding author: Longxiang Yang (yanglx@njupt.edu.cn)

This work was supported in part by the National Key Research and Development Program of China under Grant 2018YFC1314903, in part by the Natural Science Foundation of China under Grant 61861039, Grant 61372124, and Grant 61427801, in part by the Science and Technology Project Foundation of Gansu Province under Grant 18YF1GA060, and in part by the Postgraduate Research and Practice Innovation Program of Jiangsu Province under Grant SJKY19_0740.

ABSTRACT In this paper, we present the detailed rate analysis for cell-free massive multiple-input multiple-output (MIMO) systems over spatially correlated Rayleigh fading channels. Taking the realistic impairment effects of spatial channel correlation, pilot contamination, and channel estimation errors into account, the lower-bounds of the achievable rates for both the uplink and downlink are derived with the low-complexity linear processing such as matched filter and conjugate beamforming, which enable us to take cognizance of the impacts of transmitted power, and the number of access points (APs). Based on the derived rate results, the asymptotic performance analysis is then carried out. Besides, we propose the sophisticated max-min power allocation strategies taking the actual requirements into consideration to provide uniformly good service to all users. However, the objective functions of the two optimization problems are both non-concave. Fortunately, the former for uplink can be characterized as geometric programming (GP), whilst the latter for downlink merging the efficient tools of second-order-cone programming (SOCP). Lastly, the numerical results are shown to verify our analytical results and the effectiveness of the proposed max-min fairness algorithms.

INDEX TERMS Cell-free massive MIMO, channel estimation, geometric programming, max-min fairness, second-order-cone programming, spatially correlated Rayleigh fading.

I. INTRODUCTION

Flexible distributed cell-free massive multiple-input multiple-output (MIMO) technology has been received considerable attentions from both the industry and academia in recent years, due to the fact it can provide high coverage probability, spatial multiplexing, and macroscopic diversity [1]–[3]. Therefore, it has been considered as an alternative option for the most disruptive technologies towards the beyond fifth-generation (B5G) and sixth-generation (6G) mobile communication systems [4]–[7].

The concept of cell-free massive MIMO was first proposed in the seminal works [1], [2], it has been demonstrated that ten-fold improvements in the 5%-outage rate can be obtained compared with the small cells. As a new paradigm shift from the traditional massive MIMO and network MIMO, with the aid of large numbers of independently distributed setups of access points (APs), there are following distinguishing features and outstanding aspects: (*a*) it can avoid excessive inter-cell handover, reduce control signaling interaction in conjunction with believably improve radio resource utilization due to the fact that there are no cells or boundaries [2]; (*b*) the AP in the cell-free massive MIMO systems only needs to obtain the local channel state information (CSI)[1] for data transmission but does not need to exchange the instantaneous CSI through the backhaul link, which can greatly reduce the serious overhead of the fronthaul link resources [4], [6]; (*c*) the distributed APs will substantially reduce the average distance between the users and APs, which can reduce the effect of detrimental shading. Besides, it can also provide remarkable spatial multiplexing and huge spatial macro diversity gain [7], [8]; (*d*) with the aid of the low-complexity linear processing, it also can inherit the excellent transmission characteristics, such as the effect channel hardening

The associate editor coordinating the review of this manuscript and approving it for publication was Rui Wang.

[1]In general, local CSI indicates the channel between all APs and users, which can be obtained with time diversion duplexing (TDD) protocol.

phenomena and the asymptotically favorable propagation conditions, which will effectively mitigate or eliminate the multi-users interference completely [9].

A. LITERATURE REVIEW

With the advantages shown above, in recent years, cell-free massive MIMO has been extensively studied [10]–[15]. Different from the legacy precoding schemes as [2] which can suppress intra-cell interference only, a full-pilot zero-forcing scheme is proposed in [11]. Based on this, in [12], the downlink spectral efficiency (SE) and max-min fairness optimization were discussed under imperfect CSI. Besides, with the fact that the multiple users can be served at the same resource block with non-orthogonal multiple access (NOMA), the NOMA-aided downlink cell-free massive MIMO was firstly considered in [13], in which all users are divided into multiple clusters. In virtue of all users in the same clusters use the same pilot, therefore, the numerical results show that the served users by NOMA significantly higher than the orthogonal multiple access (OMA) ones, and the achievable sum rate exceed the OMA as well in the regime of a low number of users. With this contribution, the work in [14] considers the scenario of multi-antenna AP, and proposed the rate maximization algorithm. Besides the derived insight as [11], it further showed that the original problem can be effectively solved by sequential convex approximation (SCA). Moreover, for maximizing the average per-user bandwidth efficiency of the cell-free massive MIMO system, the adaptive NOMA/ OMA mode-switching method was proposed in [15].

The excellent performance for the above-mentioned works is under the common assumption that the uncorrelated Rayleigh channel. However, due to the fact that large numbers of antennas are equipped at each AP, in the real cell-free massive MIMO systems, the actual transmission channel is always spatially correlated owing to the multiple antennas are mounted in a limited physical space and the poor scattering conditions.[2] Therefore, it is necessary to study the spatial correlation for the seminal cell-free massive MIMO systems. During the past few years, the spatial correlation has been received much attention in massive MIMO systems [16]–[18]. For example, the authors in [17] analyze the achievable rate, energy efficiency (EE), and also study the trade-off for the mixed analog-to-digital converter (ADC) massive MIMO relaying systems over spatially correlated channels.

While the spatial correlation is well-studied in recent years, as far as the authors concern, it has not been received much attention in the seminal cell-free massive MIMO system yet. Only very in recently, with the least-square estimator, the authors in [19] investigated the uplink performance for cell-free massive MIMO over spatially correlated Rayleigh fading without any power allocation scheme. However, this work is not thorough, and it is deserved to further deeply analyze and investigate.

[2]Since the large numbers of antennas in the distributed APs have non-uniform radiation patterns, and the physical propagation environment makes certain spatial directions more likely to carry strong signals than other directions, therefore, the spatial correlated fading is very important for large arrays since these have a good spatial resolution than the number of scattering clusters [20].

B. SPECIAL CONTRIBUTIONS

In this work, we consider a spatially correlated Rayleigh fading channel for cell-free massive MIMO system, in which the matched filtering for uplink and conjugate beamforming for downlink are implemented. To the best of authors' knowledge, this is the first one to consider the impact of the spatial channel relevance for a cell-free massive MIMO system with the effect of pilot contamination.

Motivated by the above considerations, the main contributions of this paper are elaborated as follows:

1) Under imperfect CSI scenarios, the statistical properties of the estimated channel and channel error are derived by virtue of the standard minimum mean squared error (MMSE) channel estimation technique, which can be used to perform multiplexing/ de-multiplexing operation.
2) With the matched filtering and conjugate beamforming, the rigorous closed-form rate expressions are derived. Leveraging on the asymptotic arguments, we can characterize the impact of transmitted power, and the number of APs.
3) Based on the derived rates, moreover, the asymptotic performance analysis are then carried out. The results show that the inter-user interference and the additive noise will disappear when the numbers of APs go to infinite. Only the desired signal and the pilot contamination part are reserved.
4) In order to effectively tackle the poor user fairness issue caused by different users' geographic locations, the sophisticated max-min fairness power allocation schemes are designed based on the derived rate expressions. Considering the fact that the proposed schemes are difficult to solve, fortunately, it can be characterized by geometric programming (GP) for the uplink, while the one for the downlink is second-order-cone programming (SOCP), respectively.

C. OUTLINE

The remainder of this paper is organized as follows. Section II describes the cell-free massive MIMO system model under spatially correlated Rayleigh fading channels. With the matched filtering and conjugate beamforming, section III derives the rate expressions under imperfect CSI scenarios. Besides, the asymptotic performance analyses are provided in Section IV. After that, Section V considers the max-min power allocation strategies based on the derived closed-form rate expressions. Moreover, Section VI presents the performance evaluation to verify our derived results and finally, the conclusion marks are given in Section VII.

D. NOTATION

For notational convenience, in this paper, upper-case boldface and lower-case boldface letters are denoted by matrices and

column vectors. Otherwise stated, $\mathbf{A}^*$, $\mathbf{A}^T$, and $\mathbf{A}^H$ stand for the conjugate, transpose, and conjugate transpose of the matrix $\mathbf{A}$, respectively. Besides, $\mathrm{tr}(\cdot)$, $\mathbb{V}\mathrm{ar}(\cdot)$, and $\mathbb{E}\{\cdot\}$ stand for the trace, variance, and expectation operations, whilst $\mathbf{I}_N$ denotes the $N \times N$ identity matrix. Moreover, $|\cdot|$ and $\|\cdot\|$ indicate the absolute and Euclidean norm operations. Finally, $\mathcal{N}_{\mathbb{C}}(\mathbf{0}, \mathbf{R})$ represents the circularly symmetric complex Gaussian distribution with zero mean vector and the standard deviation with spatial correlation matrix $\mathbf{R}$.

II. SYSTEM MODEL AND PRELIMINARIES

In this work, under spatially correlated Rayleigh fading channels, we consider a cell-free massive MIMO system consisting of M distributed APs equipped with N antennas coherently serve K single-antenna mobile users. Assuming that all users simultaneously transmit their signals to the APs in the uplink phase, given that the N-dimensional received signal, $\mathbf{y}_m \in \mathbb{C}^{N\times 1}$, at the m-th AP is generally modeled as

$$\mathbf{y}_m = \mathbf{G}_m \mathbf{P}^{1/2}\mathbf{x} + \mathbf{n}_m, \tag{1}$$

where $\mathbf{G}_m = \left[\mathbf{g}_{m1}, \mathbf{g}_{m2}, \ldots, \mathbf{g}_{mK}\right] \in \mathbb{C}^{N\times K}$ denotes the channel matrix from the m-th AP to all K users. Besides, $\mathbf{P}$ indicates a diagonal matrix with $[\mathbf{P}]_{kk} = \rho\eta_k$, where the factor ρ corresponds to the power of the transmitted signal, $0 \le \eta_k \le 1, \forall k$, is the power allocation coefficient for the k-th user, and $\mathbf{x} \in \mathbb{C}^{K\times 1}$ represents the corresponding transmitted signal of all users. Besides, the vector $\mathbf{n}_m \sim \mathcal{N}_{\mathbb{C}}(\mathbf{0}, \mathbf{I}_N)$ denotes the additive white Gaussian noise (AWGN) vector at the m-th AP. In contrast to [5]–[8], [21], we advocate the more realistic spatially correlated Rayleigh fading channels [19]. Specifically, the correlated Rayleigh channel vector between the k-th user and the m-th AP can be modeled as [20]

$$\mathbf{g}_{mk} \sim \mathcal{N}_{\mathbb{C}}(\mathbf{0},\ \mathbf{R}_{mk}), \tag{2}$$

where $\mathbf{R}_{mk} \in \mathbb{C}^{N\times N}$ denotes the positive semi-definite spatial correlation matrix[3] reflecting the effects of macroscopic propagation, which is generally not diagonal and assumed to be known in advance at the m-th AP. For the covariance matrix $\mathbf{R}_{mk}$, it advocates the local scattering spatial correlation model with Gaussian angular distribution, where the (p, q)-th entry of $\mathbf{R}_{mk}$ is thus given by

$$[\mathbf{R}_{mk}]_{p,q} = \beta_{mk}\int_{-20\sigma_\varphi}^{20\sigma_\varphi} \mathrm{e}^{2\pi j \mathrm{d}_H (p-q)\sin(\phi+\delta)} \frac{1}{\sqrt{2\pi}\sigma_\varphi} \mathrm{e}^{-\frac{\delta^2}{2\sigma_\varphi^2}} \mathrm{d}\delta, \tag{3}$$

where β_{mk} denotes the large-scale fading coefficient, d_H represents the antenna spacing, and ϕ indicates a deterministic nominal angel. Besides, the factor $\delta \sim \mathcal{N}_{\mathbb{C}}(0,\ \sigma_\varphi)$ refers to a random deviation from the nominal angle, where σ_φ means the angular standard deviation (ASD). From (3), we find $\mathbf{R}_{mk}$ is in general not diagonal. When $\mathbf{R}_{mk} = \beta_{mk}\mathbf{I}_N$, thus it becomes a special uncorrelated Rayleigh fading.

[3]The Hermitian matrix $\mathbf{R}_{mk}$ is positive semi-definite if and only-if its eigenvalues are non-negative, and it is not diagonal in general. It reflects the effect of large-scale antenna gains, radiation patterns, and so on.

Assuming that the TDD operation is proceed, we can utilize channel reciprocity to acquire the downlink CSI by virtue of the uplink CSI.[4] For each coherence interval, it is composed by the following three phases, *i.e.*, uplink pilot training, uplink data transmission, and downlink data transmission phases.

A. UPLINK PILOT TRAINING

In general, sufficient accurate channel estimation is of paramount importance with each resource block. It has far-reaching effects on accurate signal detection and effective precoding. In this section, we herein assume that all users use the pre-allocated pilot sequences to the APs for uplink pilot training. Then, the received pilot signal at the m-th AP is given as

$$\mathbf{Y}_{m,\mathrm{p}} = \sqrt{\tau\rho_\mathrm{p}}\sum_{k=1}^{K}\mathbf{g}_{mk}\boldsymbol{\varphi}_k^H + \mathbf{N}_{m,\mathrm{p}}, \tag{4}$$

where τ denotes the length of pilot sequence, ρ_p represents the transmitted power of the pilot symbol. In addition, $\boldsymbol{\varphi}_k \in \mathbb{C}^{\tau\times 1}$ indicates the pilot signal assigned to the k-th user, which satisfies $\left\|\boldsymbol{\varphi}_k\right\|^2 = 1$. Besides, $\mathbf{N}_{m,\mathrm{p}}$ refers to the AWGN matrix with the (n, ς)-th entry distributed as $\left[\mathbf{N}_{m,\mathrm{p}}\right]_{n,\varsigma} \sim \mathcal{N}_{\mathbb{C}}(0,\ 1)$. In this paper, we assume $K > \tau$ and define the set $\mathcal{P}_k$ stand for, for simplicity, the users that utilize the identical pilot sequences as user k.

Based on the observable pilot matrix, the m-th AP correlates $\mathbf{Y}_{m,\mathrm{p}}$ with the pilot sequence $\boldsymbol{\varphi}_k$, leading to

$$\breve{\mathbf{y}}_{mk,\mathrm{p}} = \mathbf{Y}_{m,\mathrm{p}}\boldsymbol{\varphi}_k = \sqrt{\tau\rho_\mathrm{p}}\sum_{k'\in\mathcal{P}_k}\mathbf{g}_{mk'} + \mathbf{N}_{m,\mathrm{p}}\boldsymbol{\varphi}_k. \tag{5}$$

With the $\breve{\mathbf{y}}_{mk,\mathrm{p}}$, we can obtain the following lemma, which shows the statistical properties of the estimated channel and channel error.

Lemma 1: For the considered spatially correlated Rayleigh channels, the minimum mean square error (MMSE) estimate of channel gain $\mathbf{g}_{mk}$ in terms of $\breve{\mathbf{y}}_{mk,\mathrm{p}}$ can be given as [22]

$$\hat{\mathbf{g}}_{mk} = \sqrt{\tau\rho_\mathrm{p}}\mathbf{R}_{mk}\boldsymbol{\Xi}_{mk}\breve{\mathbf{y}}_{mk,\mathrm{p}}, \tag{6}$$

where $\boldsymbol{\Xi}_{mk}$ is written as

$$\boldsymbol{\Xi}_{mk} = \left(\tau\rho_\mathrm{p}\sum_{k'\in\mathcal{P}_k}\mathbf{R}_{mk'} + \mathbf{I}_N\right)^{-1}. \tag{7}$$

From (6) we can know that the estimated channel is degraded not only by the noise but also by the effect of pilot contamination. Besides, the MMSE estimated channel $\hat{\mathbf{g}}_{mk}$ and the corresponding estimation error $\tilde{\mathbf{g}}_{mk}$ are complex Gaussian random vectors, distributed as follows

$$\hat{\mathbf{g}}_{mk} \sim \mathcal{N}_{\mathbb{C}}(\mathbf{0},\ \mathbf{Q}_{mk}), \tag{8}$$

$$\tilde{\mathbf{g}}_{mk} \sim \mathcal{N}_{\mathbb{C}}(\mathbf{0}, \mathbf{C}_{mk}), \tag{9}$$

[4]With TDD protocol, the local CSI, which indicates that the channel between the AP and each of the users, can be obtained conveniently. Therefore, the overhead of the pilot resource is independent of the numbers of APs [9].

where $\mathbf{Q}_{mk} = \mathbf{R}_{mk} - \mathbf{C}_{mk}$ and $\mathbf{C}_{mk}$ can be expressed as

$$\mathbf{C}_{mk} = \mathbf{R}_{mk} - \tau \rho_{\mathrm{p}} \mathbf{R}_{mk} \boldsymbol{\Xi}_{mk} \mathbf{R}_{mk}. \tag{10}$$

Proof: See Appendix A.

B. UPLINK DATA TRANSMISSION

In the uplink phase, we assume that all K users simultaneously transmit data to the APs and different users utilize different transmitted powers, with power control coefficient η_k ruling the power transmitted by the m-th AP, $0 \leq \eta_k \leq 1, \forall k$. Before sending the data, the k-th user weights its symbol q_k, $\mathbb{E}\left\{|q_k|^2\right\} = 1$. Then the received analog signal at the m-th AP can be given as

$$\mathbf{y}_{m,\mathrm{u}} = \sqrt{\rho_{\mathrm{u}}} \sum_{k=1}^{K} \sqrt{\eta_k} \mathbf{g}_{mk} q_k + \mathbf{n}_{m,\mathrm{u}}, \tag{11}$$

where ρ_{u} refers to the maximum transmitted power constraint and $\mathbf{n}_{m,\mathrm{u}} \sim \mathcal{N}_{\mathbb{C}}(\mathbf{0}, \mathbf{I}_N)$ denotes the AWGN.

In this paper, a low-complexity linear processing matched filtering technique is advocated in the uplink to correlate $\mathbf{y}_{m,\mathrm{u}}$ for detecting the delivered signal q_k, which can be easily employed in a distributed manner at each AP. Specifically, the m-th AP multiplies $\mathbf{y}_{m,\mathrm{u}}$ with estimated channels coefficient $\hat{\mathbf{g}}_{mk}^H$, yielding

$$\begin{aligned} y_{mk,\mathrm{u}} &= \hat{\mathbf{g}}_{mk}^H \mathbf{y}_{m,\mathrm{u}} \\ &= \sqrt{\rho_{\mathrm{u}}} \sum_{k'=1}^{K} \sqrt{\eta_{k'}} \hat{\mathbf{g}}_{mk}^H \mathbf{g}_{mk'} q_{k'} + \hat{\mathbf{g}}_{mk}^H \mathbf{n}_{m,\mathrm{u}}. \end{aligned} \tag{12}$$

After the m-th AP sending $y_{mk,\mathrm{u}}$ to the central processing unit (CPU) via the fronthaul network, the sum received signals at the CPU can be expressed as

$$\begin{aligned} r_{k,\mathrm{u}} &= \sum_{m=1}^{M} \hat{\mathbf{g}}_{mk}^H \mathbf{y}_{m,\mathrm{u}} \\ &= \sqrt{\rho_{\mathrm{u}}} \sum_{m=1}^{M} \sum_{k'=1}^{K} \sqrt{\eta_{k'}} \hat{\mathbf{g}}_{mk}^H \mathbf{g}_{mk'} q_{k'} + \sum_{m=1}^{M} \hat{\mathbf{g}}_{mk}^H \mathbf{n}_{m,\mathrm{u}}. \end{aligned} \tag{13}$$

Then q_k can be detected from $r_{k,u}$.

C. DOWNLINK DATA TRANSMISSION

The APs treat the estimated channels as the real channels after the phase of uplink pilot training. In this phase, the APs precode the data signals intended for all users by virtue of the conjugate beamforming precoder. The precoded signal at the m-th AP is formulated as

$$\mathbf{x}_m = \sqrt{\rho_{\mathrm{d}}} \sum_{k=1}^{K} \sqrt{\eta_{mk}} \hat{\mathbf{g}}_{mk}^* s_k, \tag{14}$$

where ρ_{d} indicates the maximum downlink transmit power, $\eta_{mk}, \forall m, \forall k$ refers to a scalar power control coefficient ruling the transmitted power by the m-th AP for the k-th user, and $s_k \sim \mathcal{N}_{\mathbb{C}}(0, 1)$ denotes the data signal intended for the k-th user.

With the signal given in (14), the transmitted power of the m-th AP can be given as

$$\mathbb{E}\left\{\|\mathbf{x}_m\|^2\right\} = \rho_{\mathrm{d}} \sum_{k=1}^{K} \eta_{mk} \mathrm{tr}\left(\mathbf{Q}_{mk}\right). \tag{15}$$

To satisfy the power constraint at the m-th AP, the power control coefficients need to satisfy the following equation

$$\sum_{k=1}^{K} \eta_{mk} \mathrm{tr}\left(\mathbf{Q}_{mk}\right) \leq 1. \tag{16}$$

By virtue of (14), the received signal at the k-th user can be rewritten as

$$\begin{aligned} r_{k,\mathrm{d}} &= \sum_{m=1}^{M} \mathbf{g}_{mk}^T \mathbf{x}_m + n_{k,\mathrm{d}} \\ &= \sqrt{\rho_{\mathrm{d}}} \sum_{m=1}^{M} \mathbf{g}_{mk}^T \sum_{k'=1}^{K} \sqrt{\eta_{mk'}} \hat{\mathbf{g}}_{mk'}^* s_{k'} + n_{k,\mathrm{d}}, \end{aligned} \tag{17}$$

where $n_{k,\mathrm{d}}$ is the $\mathcal{N}_{\mathbb{C}}(0, 1)$ AWGN.

III. RATE PERFORMANCE ANALYSIS

This section investigates the anticipated rate performance analysis in terms of the rigorous uplink and downlink rate expressions [8], for cell-free massive MIMO system with matched filtering receiver and conjugate beamforming precoder over spatially correlated Rayleigh fading channel. The obtained closed-form expressions account for the effect of channel estimation errors and pilot contamination. Furthermore, leveraging on the asymptotic arguments, we provide some novel insights about the key system parameters.

A. ACHIEVABLE UPLINK RATE

From (13), $r_{k,\mathrm{u}}$ can be further reformulated as

$$r_{k,\mathrm{u}} = \underbrace{\sqrt{\rho_{\mathrm{u}} \eta_k} \mathbb{E}\left\{\sum_{m=1}^{M} \hat{\mathbf{g}}_{mk}^H \mathbf{g}_{mk}\right\} q_k}_{\text{desired signal}} + \underbrace{w_{k,\mathrm{u}}}_{\text{additive noise}} \tag{18}$$

where $w_{k,\mathrm{u}}$ representing the additive noise is denoted by

$$\begin{aligned} w_{k,\mathrm{u}} &= \underbrace{\sqrt{\rho_{\mathrm{u}} \eta_k} \left(\sum_{m=1}^{M} \hat{\mathbf{g}}_{mk}^H \mathbf{g}_{mk} - \mathbb{E}\left\{\sum_{m=1}^{M} \hat{\mathbf{g}}_{mk}^H \mathbf{g}_{mk}\right\}\right) q_k}_{\text{beamforming gain uncertainty}} \\ &\quad + \underbrace{\sqrt{\rho_{\mathrm{u}}} \sum_{k' \neq k}^{K} \sqrt{\eta_{k'}} \sum_{m=1}^{M} \hat{\mathbf{g}}_{mk}^H \mathbf{g}_{mk'} q_{k'}}_{\text{inter-user interference}} + \underbrace{\sum_{m=1}^{M} \hat{\mathbf{g}}_{mk}^H \mathbf{n}_{m,\mathrm{u}}}_{\text{thermal noise}}. \end{aligned} \tag{19}$$

Assuming $w_{k,\mathrm{u}}$ is uncorrelated with q_k and applying the philosophy that uncorrelated Gaussian noise yields a capacity lower bound [2], therefore, this assumption allows us to

derive the uplink lower bound of the rate for the k-th user. As described earlier, the achievable uplink rate expression of the k-th user can be denoted by

$$R_{k,\mathrm{u}} = \log_2\left(1 + \frac{A_k}{B_{1k} + B_{2k} + B_{3k}}\right), \tag{20}$$

where A_k, B_{1k}, B_{2k}, and B_{3k} can be respectively given as

$$A_k = \rho_\mathrm{u}\eta_k \left|\mathbb{E}\left\{\sum_{m=1}^{M} \hat{\mathbf{g}}_{mk}^H \mathbf{g}_{mk}\right\}\right|^2, \tag{21}$$

$$B_{1k} = \rho_\mathrm{u}\eta_k \mathbb{V}\mathrm{ar}\left(\sum_{m=1}^{M} \hat{\mathbf{g}}_{mk}^H \mathbf{g}_{mk}\right), \tag{22}$$

$$B_{2k} = \rho_\mathrm{u} \sum_{k'\neq k}^{K} \eta_{k'} \mathbb{E}\left\{\left|\sum_{m=1}^{M} \hat{\mathbf{g}}_{mk}^H \mathbf{g}_{mk'}\right|^2\right\}, \tag{23}$$

$$B_{3k} = \mathbb{E}\left\{\left|\sum_{m=1}^{M} \hat{\mathbf{g}}_{mk}^H \mathbf{n}_{m,\mathrm{u}}\right|^2\right\}. \tag{24}$$

Theorem 1: For the considered spatially correlated Rayleigh fading, an achievable uplink rate expression of the k-th user with matched filtering receiver is formulated as (20), where A_k, B_{1k}, B_{2k}, and B_{3k} can be calculated as

$$A_k = \rho_\mathrm{u}\eta_k \left(\sum_{m=1}^{M} \mathrm{tr}\left(\mathbf{Q}_{mk}\right)\right)^2, \tag{25}$$

$$B_{1k} = \rho_\mathrm{u}\eta_k \sum_{m=1}^{M} \mathrm{tr}\left(\mathbf{R}_{mk}\left(\mathbf{Q}_{mk}\right)\right), \tag{26}$$

$$B_{2k} = \tau^2\rho_\mathrm{p}^2\rho_\mathrm{u} \sum_{k'\in\mathcal{P}_k\setminus\{k\}} \eta_{k'} \left|\sum_{m=1}^{M} \mathrm{tr}\left(\mathbf{R}_{mk'}\mathbf{R}_{mk}\boldsymbol{\Xi}_{mk}\right)\right|^2 + \rho_\mathrm{u} \sum_{k'\neq k}^{K} \eta_{k'} \sum_{m=1}^{M} \mathrm{tr}\left(\mathbf{R}_{mk'}\left(\mathbf{Q}_{mk}\right)\right), \tag{27}$$

$$B_{3k} = \sum_{m=1}^{M} \mathrm{tr}\left(\mathbf{Q}_{mk}\right). \tag{28}$$

Proof: See Appendix B.

In Theorem 1, we present an exact closed-form uplink rate expression for the considered cell-free massive MIMO system over spatially correlated Rayleigh fading, which enables us to further evaluate the impact of the key system parameters on the achieved sum rate.

Remark 1: In fact, the derived results given in Theorem 1 is general, when $\mathbf{R}_{mk} = \beta_{mk}\mathbf{I}_N$, the derived results in Theorem 1 can be reduced to the uncorrelated Rayleigh fading. Thus, it can be simplified as [2]

$$R_{k,\mathrm{u}}^{\text{Unco-Ray}} = \log_2\left(1 + \frac{\bar{A}_k}{\bar{B}_{1k} + \bar{B}_{2k} + \bar{B}_{3k}}\right), \tag{29}$$

where the superscript "Unco-Ray" stands for "Uncorrelated Rayleigh fading". Besides, $\bar{A}_k, \bar{B}_{1k}, \bar{B}_{2k}$, and $\bar{B}_{3k}$ can be respectively denoted by

$$\bar{A}_k = \rho_\mathrm{u}\eta_k N^2 \left(\sum_{m=1}^{M} \gamma_{mk}\right)^2, \tag{30}$$

$$\bar{B}_{1k} = N^2\rho_\mathrm{u} \sum_{k'\in\mathcal{P}_k\setminus\{k\}} \eta_{k'} \left(\sum_{m=1}^{M} \frac{\beta_{mk'}}{\beta_{mk}}\right)^2, \tag{31}$$

$$\bar{B}_{2k} = N^2\rho_\mathrm{u} \sum_{k'\in\mathcal{P}_k} \eta_{k'} \sum_{m=1}^{M} \gamma_{mk}^2 \frac{\beta_{mk'}^2}{\beta_{mk}^2}, \tag{32}$$

$$\bar{B}_{3k} = N \sum_{m=1}^{M} \gamma_{mk}, \tag{33}$$

where γ_{mk} is defined by

$$\gamma_{mk} = \frac{\tau\rho_\mathrm{p}\beta_{mk}^2}{\tau\rho_\mathrm{p} \sum_{k'\in\mathcal{P}_k} \beta_{mk'} + 1}. \tag{34}$$

The derived result is identical to the achievable rate for a cell-free massive MIMO system with uncorrelated Rayleigh fading scenario [2, Eq. (27)].

Thus, the uplink sum rate of the cell-free massive MIMO system over spatially correlated Rayleigh fading is

$$R_\mathrm{u}^{\mathrm{sum}} = \sum_{k=1}^{K} R_{k,\mathrm{u}}. \tag{35}$$

Remark 2: The derived approximate result in theorem 1 is very tight to the case when the CSI is perfectly known at all APs. With (17), the "ergodic" rate formula of the k-th user with genie-aided CSI is formulated as

$$R_{k,\mathrm{u}}^{\mathrm{erg}} = \mathbb{E}\left\{\log_2\left(1 + \mathrm{SINR}_{k,\mathrm{u}}^{\mathrm{erg}}\right)\right\}, \tag{36}$$

where the superscript "erg" stands for "ergodic" and

$$\mathrm{SINR}_{k,\mathrm{u}}^{\mathrm{erg}} = \frac{\rho_\mathrm{u}\eta_k \left|\sum_{m=1}^{M} \hat{\mathbf{g}}_{mk}^H \mathbf{g}_{mk}\right|^2}{\rho_\mathrm{u} \sum_{k'\neq k}^{K} \eta_{k'} \left|\sum_{m=1}^{M} \hat{\mathbf{g}}_{mk}^H \mathbf{g}_{mk'}\right|^2 + \left|\sum_{m=1}^{M} \hat{\mathbf{g}}_{mk}^H \mathbf{n}_{m,\mathrm{u}}\right|^2}. \tag{37}$$

Note that the genie-aided CSI will be used in the Section VI to verify the effectiveness of our derivation.

B. ACHIEVABLE DOWNLINK RATE

Following the same methodology as theorem 1, we now provide the rigorous achievable downlink rate expression for the k-th user.

Theorem 2: For the considered spatially correlated Rayleigh fading, an achievable downlink rate expression of the k-th user with conjugate beamforming precoder is characterized by

$$R_{k,\mathrm{d}} = \log_2\left(1 + \frac{C_k}{D_{1k} + D_{2k} + 1}\right), \tag{40}$$

where C_k, D_{1k}, and D_{2k} can be respectively expressed as

$$C_k = \rho_{\mathrm{d}} \left(\sum_{m=1}^{M} \sqrt{\eta_{mk}} \mathrm{tr}\left(\mathbf{Q}_{mk}\right) \right)^2, \tag{41}$$

$$D_{1k} = \tau^2 \rho_{\mathrm{p}}^2 \rho_{\mathrm{d}} \sum_{k' \in \mathcal{P}_k \setminus \{k\}} \left(\sum_{m=1}^{M} \sqrt{\eta_{mk'}} \mathrm{tr}\left(\mathbf{R}_{mk} \mathbf{R}_{mk'} \boldsymbol{\Xi}_{mk'}\right) \right)^2, \tag{42}$$

$$D_{2k} = \rho_{\mathrm{d}} \sum_{k'=1}^{K} \sum_{m=1}^{M} \eta_{mk'} \mathrm{tr}\left(\mathbf{R}_{mk} \left(\mathbf{Q}_{mk'}\right)\right). \tag{43}$$

Remark 3: Similar to the remark 1, the derived results in theorem 2 also can be reduced to the uncorrelated Rayleigh fading case when $\mathbf{R}_{mk} = \beta_{mk} \mathbf{I}_N$. Thus, (40) can be simplified as

$$R_{k,\mathrm{d}}^{\text{Unco-Ray}} = \log_2 \left(1 + \frac{\bar{C}_k}{\bar{D}_{1k} + \bar{D}_{2k} + 1} \right), \tag{44}$$

where $\bar{C}_k$, $\bar{D}_{1k}$, and $\bar{D}_{2k}$ can be respectively given by

$$\bar{C}_k = N^2 \rho_{\mathrm{d}} \left(\sum_{m=1}^{M} \sqrt{\eta_{mk}} \gamma_{mk} \right)^2, \tag{45}$$

$$\bar{D}_{1k} = N^2 \rho_{\mathrm{d}} \sum_{k' \in \mathcal{P}_k \setminus \{k\}} \left(\sum_{m=1}^{M} \sqrt{\eta_{mk'}} \gamma_{mk'} \frac{\beta_{mk}}{\beta_{mk'}} \right)^2, \tag{46}$$

$$\bar{D}_{2k} = N \rho_{\mathrm{d}} \sum_{k'=1}^{K} \sum_{m=1}^{M} \eta_{mk'} \gamma_{mk'} \beta_{mk}. \tag{47}$$

The resulting finding in remark 3 is the consequence of the downlink rate bound of a cell-free massive MIMO system with uncorrelated Rayleigh fading obtained in [2, Eq. (24)].

Thus, the downlink sum rate of the considered cell-free massive MIMO system over spatially correlated Rayleigh fading is given as

$$R_{\mathrm{d}}^{\mathrm{sum}} = \sum_{k=1}^{K} R_{k,\mathrm{d}}. \tag{48}$$

IV. ASYMPTOTIC PERFORMANCE ANALYSIS

By the continuous Mapping theorem and Chebyshev's theorem [23], we first present the following lemma for the arbitrary spatial correlation matrices before we continue.

Lemma 2: The spatial correlation matrix $\mathbf{R}_{mk}, m = 1, 2, \ldots, M, k = 1, 2, \ldots, K$, satisfies [20]

$$\limsup_{M} \|\mathbf{R}_{mk}\|_2 < \infty, \tag{49}$$

$$\liminf_{M} \frac{1}{M} \mathrm{tr}\left(\mathbf{R}_{mk}\right) > 0. \tag{50}$$

With the aid of the above lemma 2, in this section we present the asymptotic performance analysis for both the uplink and downlink.

A. UPLINK ASYMPTOTIC ANALYSIS

Theorem 3: The asymptotic analysis for the downlink rate can be given as follows (38), as shown at the bottom of this page, where "$p_n \asymp q_n$" denotes the equivalence relation $p_n - q_n \xrightarrow[n\to\infty]{\text{a.s.}} 0$ for two infinite sequences p_n and q_n.

Proof: See Appendix C.

B. DOWNLINK ASYMPTOTIC ANALYSIS

Theorem 4: Proceeding similarly as for the uplink case, the asymptotic analysis for the downlink rate can be given as (39), which can be found at the bottom of this page.

Proof: Similar to the uplink, the proof of the downlink asymptotic analysis can be achieved and thus omitted.

V. PROPOSED MAX-MIN POWER CONTROL SCHEMES

Taking the fairness between the different users with different graphical locations into consideration, in the section, the max-min power control schemes for both uplink and downlink are then proceeded for pursuing a detailed investigation, separately. All the APs are involved in serving a typical user coherently. These proposed power control schemes are meant to be governed by the collective CPU, which is capable of guaranteeing the max-min fairness by calculating the large scale coefficients $\beta_{mk}, m = 1, 2, \ldots, M, k = 1, 2, \ldots, K$.

A. MAX-MIN FAIRNESS FOR UPLINK

For the case that cell-free system under spatially correlated Rayleigh fading channels, mathematically, the max-min power control algorithm subjecting to the power constraints for the uplink can be formulated as

$$P_1: \max_{\{\eta_k\}} \min_{k=1,2,\ldots,K} R_{k,\mathrm{u}}\left(\eta_k\right) \tag{52a}$$

$$\text{s.t.} 0 \le \eta_k \le 1, \quad k = 1, 2, \ldots, K. \tag{52b}$$

$$\frac{r_{k,\mathrm{u}}}{M} \asymp \frac{\tau \rho_{\mathrm{p}} \sqrt{\rho_{\mathrm{u}}}}{M} \left(\sqrt{\eta_k} \sum_{m=1}^{M} \mathrm{tr}\left(\mathbf{R}_{mk} \boldsymbol{\Xi}_{mk} \mathbf{R}_{mk}\right) - \sum_{k' \neq k}^{K} \sqrt{\eta_{k'}} \sum_{m=1}^{M} \mathrm{tr}\left(\mathbf{R}_{mk} \boldsymbol{\Xi}_{mk} \mathbf{R}_{mk'}\right) \boldsymbol{\varphi}_{k'}^H \boldsymbol{\varphi}_k \right) \tag{38}$$

$$\frac{r_{k,\mathrm{d}}}{M} \asymp \frac{\tau \rho_{\mathrm{p}} \sqrt{\rho_{\mathrm{d}}}}{M} \left(\sum_{m=1}^{M} \sqrt{\eta_{mk}} \mathrm{tr}\left(\mathbf{R}_{mk} \mathbf{R}_{mk} \boldsymbol{\Xi}_{mk}\right) - \sum_{k' \neq k}^{K} \sum_{m=1}^{M} \sqrt{\eta_{mk'}} \mathrm{tr}\left(\mathbf{R}_{mk} \mathbf{R}_{mk'} \boldsymbol{\Xi}_{mk'}\right) \boldsymbol{\varphi}_k^T \boldsymbol{\varphi}_{k'}^* \right) \tag{39}$$

where $R_{k,\mathrm{u}}$ with respect to $\{\eta_k\}$ is defined in Theorem 1. To circumvent the challenge that the $\min(\cdot)$ is a non-differentiable objective function, by introducing a slack variable t, the original optimization problem P_1 can be equivalently transformed into

$$P_2: \max_{\{t,\eta_k\}} t \tag{53a}$$
$$\text{s.t. } t \le R_{k,\mathrm{u}}(\eta_k), \quad k = 1, 2, \ldots, K, \tag{53b}$$
$$0 \le \eta_k \le 1, \quad k = 1, 2, \ldots, K. \tag{53c}$$

Theorem 5: The uplink max-min power control problem P_2 for spatially correlated Rayleigh fading cell-free massive MIMO system is a standard GP, therefore, the standard convex solvers such as CVX can be used to solve the optimal solution.

Proof: See Appendix D.

B. MAX-MIN FAIRNESS FOR DOWNLINK

Following similar arguments as for the uplink scenario, the downlink max-min fairness algorithm can be efficiently addressed as a SOCP. Following the similar steps as the uplink and recalling (40), the downlink max-min power control problem subject to the power constraints can be measured as

$$P_3: \max_{\{\eta_{mk}\}} \min_{k=1,2,\ldots,K} R_{k,\mathrm{d}}(\eta_{mk}) \tag{54a}$$
$$\text{s.t. } \sum_{k=1}^{K} \eta_{mk} \mathrm{tr}(\mathbf{Q}_{mk}) \le 1, \ m = 1, 2, \ldots, M, \tag{54b}$$
$$\eta_{mk} \ge 0, \quad k = 1, 2, \ldots, K, \ m = 1, 2, \ldots, M. \tag{54c}$$

where $R_{k,\mathrm{d}}$ with respect to $\{\eta_{mk}\}$ is defined in Theorem 2.

We remark P_3 is nonconvex since $R_{k,\mathrm{d}}$ is nonconvex function about $\{\eta_{mk}\}$. However, the derived downlink sum rate expression in P_3 is rather involved and is not amenable for calculation. For facilitating the further analysis, we use the notation $\xi_{mk} = \sqrt{\eta_{mk}}$ and define the following auxiliary matrices and vectors

$$\bar{\boldsymbol{\xi}}_k = [\xi_{1k}, \ldots, \xi_{Mk}]^T, \tag{55}$$
$$\mathbf{a}_k = \left[\mathrm{tr}(\mathbf{Q}_{1k}), \ldots, \mathrm{tr}(\mathbf{Q}_{Mk})\right]^T, \tag{56}$$
$$\mathbf{b}_{k'k} = [\mathrm{tr}(\mathbf{R}_{1k}\mathbf{R}_{1k'}\boldsymbol{\Xi}_{1k'}), \ldots, \mathrm{tr}(\mathbf{R}_{Mk}\mathbf{R}_{Mk'}\boldsymbol{\Xi}_{Mk'})]^T, \tag{57}$$
$$\mathbf{C}_{kk'} = \mathrm{diag}\left(\sqrt{\mathrm{tr}(\mathbf{R}_{1k}(\mathbf{Q}_{1k'}))}, \ldots, \sqrt{\mathrm{tr}(\mathbf{R}_{Mk}(\mathbf{Q}_{Mk'}))}\right). \tag{58}$$

Consequently, $R_{k,\mathrm{d}}$ can be recast as (51) shown at the bottom of this page.

In order to tackle this troublesome situation effectively, coupled with several slack variable $u_{k'k}$ and $v_{k'k}$, the original optimal problem P_3 can be transformed into the following equivalent shown as

$$P_4: \max_{\{\bar{\boldsymbol{\xi}}_k, u_{k'k}, v_{k'k}\}} \min_{\forall k} \frac{\left|\mathbf{a}_k^T \bar{\boldsymbol{\xi}}_k\right|^2}{\sum\limits_{k' \in \mathcal{P}_k \setminus \{k\}} u_{k'k}^2 + \sum\limits_{k'=1}^{K} v_{k'k}^2 + \frac{1}{\rho_{\mathrm{d}}}} \tag{59a}$$
$$\text{s.t. } \tau\rho_{\mathrm{p}} \mathbf{b}_{k'k}^T \bar{\boldsymbol{\xi}}_{k'} \le u_{k'k}, \quad \forall k' \in \mathcal{P}_k \setminus \{k\}, \tag{59b}$$
$$\left\|\mathbf{C}_{kk'} \bar{\boldsymbol{\xi}}_k\right\|^2 \le v_{k'k}^2, \quad \forall k, \ \forall k', \tag{59c}$$
$$\sum_{k=1}^{K} \xi_{mk}^2 \mathrm{tr}(\mathbf{Q}_{mk}) \le 1, \quad \forall m, \tag{59d}$$
$$\xi_{mk} \ge 0, \quad \forall k, \ \forall m. \tag{59e}$$

Theorem 6: The objective function (59a) is quasi-concave and the problem P_4 is quasi-concave.

Proof: See Appendix E.

Based on the fact that the objective function is convex and the constrains are affine, therefore, the optimization problem P_4 is a quasi-concave, which can be effectively solved by means of standard convex optimization theory. Then, an efficient algorithm based on the bisection method is stated as in Algorithm 1 shown at the top of next page.

In Algorithm 1, owing to the feasible problem $\widetilde{P}_4$ involves MK scalar real variables and $K^2 + K + M$ quadratic constraints, therefore, according to [24], the pre-iteration is $\mathcal{O}\left((MK)^2\left(K^2+K+M\right)^{2.5} + \left(K^2+K+M\right)^{3.5}\right)$.

VI. PERFORMANCE EVALUATION

In this section, we conduct the performance evaluation to validate the derived analytical results and demonstrate the effectiveness of the proposed max-min fairness power allocation schemes, which help us to highlight the insight on system performance. Unless otherwise specified, the system parameters on the considered system are employed in [2], [6].

As shown in Fig. 1, the achievable uplink sum rate versus the number of APs for both the "Analytical Result" and "Ergodic Result" are illustrated, with $M = 60, N = 10$, and ASD $= 10°$, where the "Analytical Result" is based on Theorem 1 and the "Ergodic Result" is generated by the Monte-Carlo simulation method given in (36) by averaging over 10^4 independent channels realizations. It can be readily founded, the uplink sum rate grows with the increase of the number of APs due to the fact that more APs can provide more antenna gain. Furthermore, the "Ergodic Result" and the "Analytical Result" for different K are both exact match,

$$R_{k,\mathrm{d}} = \log_2\left(1 + \frac{\left|\mathbf{a}_k^T \bar{\boldsymbol{\xi}}_k\right|^2}{\tau^2\rho_{\mathrm{p}}^2 \sum\limits_{k' \in \mathcal{P}_k \setminus \{k\}} \left|\mathbf{b}_{k'k}^T \bar{\boldsymbol{\xi}}_{k'}\right|^2 + \sum\limits_{k'=1}^{K} \left\|\mathbf{C}_{kk'} \bar{\boldsymbol{\xi}}_{k'}\right\|^2 + \frac{1}{\rho_{\mathrm{d}}}}\right) \tag{51}$$

Algorithm 1 Bisection Method for Solving P_4

Input: $M, K, N, \mathbf{Q}_{mk}, \boldsymbol{\Xi}_{mk}, \tau, \rho_{\mathrm{p}}, \rho_{\mathrm{d}}$.
Ouput: $\xi_{mk}, \forall k, \forall m$.
1) Initialize the value of μ_{l} and μ_{u}, where μ_{l} and μ_{u} are the lower and upper bounds, respectively. Given the tolerance $\varepsilon > 0$.
2) **While** $\mu_{\mathrm{u}} - \mu_{\mathrm{l}} < \varepsilon$
3) Set $\mu = (\mu_{\mathrm{l}} + \mu_{\mathrm{u}})/2$ and solve the following feasible problem $\widetilde{P}_4$:

$$\begin{cases} \left\| \left[\mathbf{x}_{1k}^T \mathbf{I}_{+\mathcal{P}_k \setminus \{k\}}, \mathbf{x}_{2k}^T \mathbf{I}_K, \sqrt{1/\rho_{\mathrm{d}}} \right]^T \right\| \leq \dfrac{1}{\sqrt{\theta}} \mathbf{a}_k^T \bar{\boldsymbol{\xi}}_k, \forall k, \\ \tau \rho_{\mathrm{p}} \mathbf{b}_{k'k}^T \bar{\boldsymbol{\xi}}_{k'} \leq u_{k'k}, \forall k' \in \mathcal{P}_k \setminus \{k\}, \\ \left\| \mathbf{C}_{kk'} \bar{\boldsymbol{\xi}}_{k'} \right\|^2 \leq v_{k'k}^2, \forall k, \forall k', \\ \sum_{k=1}^{K} \xi_{mk}^2 \mathrm{tr}(\mathbf{Q}_{mk}) \leq 1, \forall m, \\ \xi_{mk} \geq 0, \forall k, \forall m, \end{cases}$$

where $\mathbf{I}_{+\mathcal{P}_k \setminus \{k\}}$ represents the matrix consisting of the k'-th, $(k' \in \mathcal{P}_k, k' \neq k)$ column of $K \times K$ unit matrix $\mathbf{I}_K$ and $\mathbf{x}_{1k} = [u_{1k}, \ldots, u_{Kk}]^T$, $\mathbf{x}_{2k} = [v_{1k}, \ldots, v_{Kk}]^T$.
4) **If** problem $\widetilde{P}_4$ is feasible, let $\mu_{\mathrm{l}} = \mu$, go to step 2, else set $\mu_{\mathrm{u}} = \mu$.
5) **end If**
6) end While

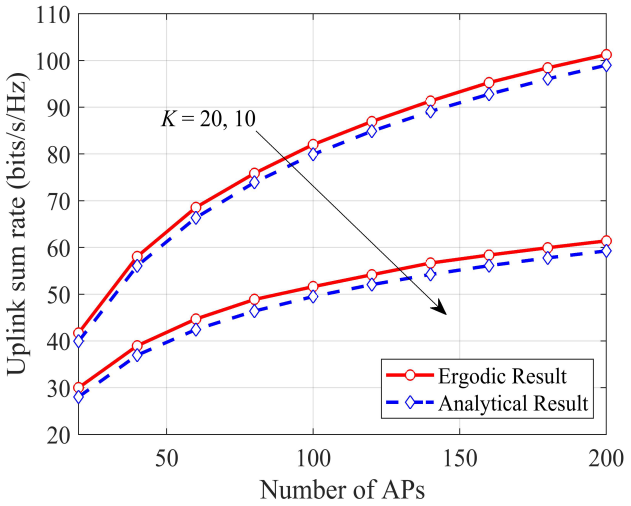

FIGURE 1. The achievable uplink sum rate versus the number of APs for both "Ergodic Result" and "Analytical Result" for different numbers of users, with $M = 60$, $N = 10$.

which confirms the validity of our derivation. Fig. 2 presents the achievable uplink sum rate versus the transmit power for different antenna configurations, with $K = 10, MN = 600$, and ASD $= 10°$. Note that the scenario "$M = 1$, $N = 600$" is response to the "centralized massive MIMO", while "$M = 60, N = 10$" corresponds to the "cell-free massive MIMO" counterpart. As we can see, in the

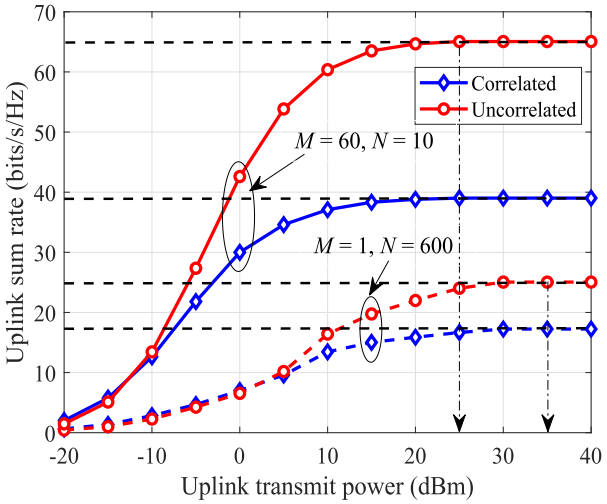

FIGURE 2. The achievable uplink sum rate versus the transmit power for different antenna configurations, with $K = 10$, $MN = 600$, and ASD $= 10°$.

low-power region, the achievable sum uplink rate rises with the increase of the transmission power. However, it saturates at the high transmission power regime. It means that when the transmission power is low, we can enhance the uplink sum rate via increasing the transmission power. Nevertheless, due to the joint effects of pilot contamination, inter-user interference, and additive noise, finally, the uplink sum rate will reach a constant value. Obviously, the case of "cell-free massive MIMO" is significantly better than the counterpart. The reason behind this is that the flexible distributed APs will greatly reduce the average distance between the users and APs, which can effectively decrease the effect of detrimental shading. Moreover, it can also provide remarkable spatial multiplexing and huge spatial macro diversity gain. When the both antenna configurations reach their maximum values, the minimum transmission power required is 25 dBm and 35 dBm, respectively.

Moreover, in the scenario of "Correlated" for both antenna configurations, we can see from that the achievable uplink sum saturation rate are 39 bits/s/Hz and 18 bits/s/Hz, which the decline rates are 41% and 28% compared with the "Uncorrelated". Obviously, we can know that the "Correlated" case severely degrades the system performance. Similar results for downlink can be obtained from Fig. 3. The decline rates for downlink are 36% and 22%, respectively. However, compared to Fig. 2, it shows that the achievable downlink sum rate is superior than the uplink case. The reason is that the downlink enjoys more power than the uplink.

In Fig. 4, the achievable uplink sum rate versus the number of APs is given, with $M = 60, K = 10$, and ASD $= 10°$. It shows that increasing the number of APs promises a enormous potential to improve the array gain. Compared with the case of "$N = 10$" and "$N = 20$", we can know that increasing the numbers of antennas at APs can bring huge

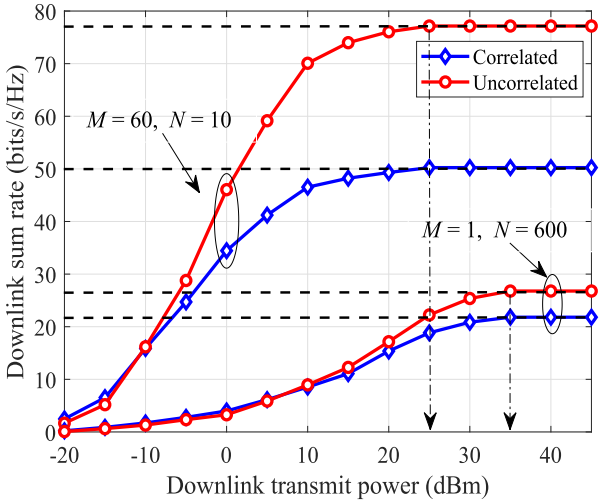

FIGURE 3. The achievable downlink sum rate versus the transmit power for different antenna configurations, with $K = 10$, $MN = 600$, and ASD = 10°.

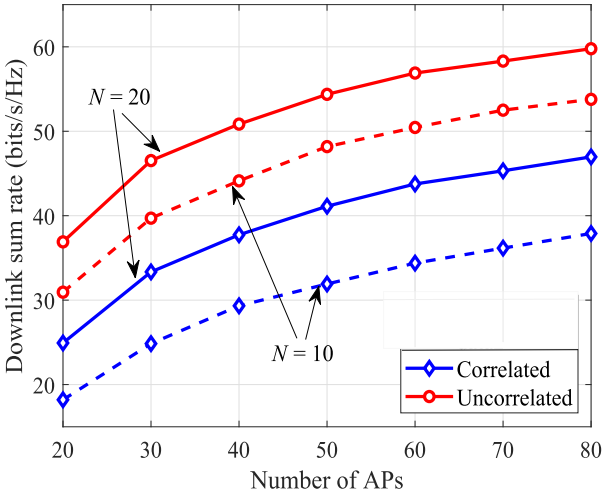

FIGURE 5. The achievable downlink sum rate versus the number of APs for different numbers of users, with $M = 60$, $K = 10$.

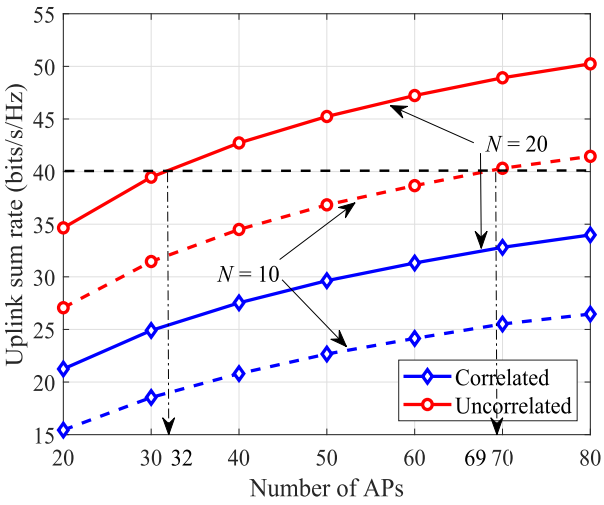

FIGURE 4. The achievable uplink sum rate versus the number of APs for different numbers of users, with $M = 60$, $K = 10$.

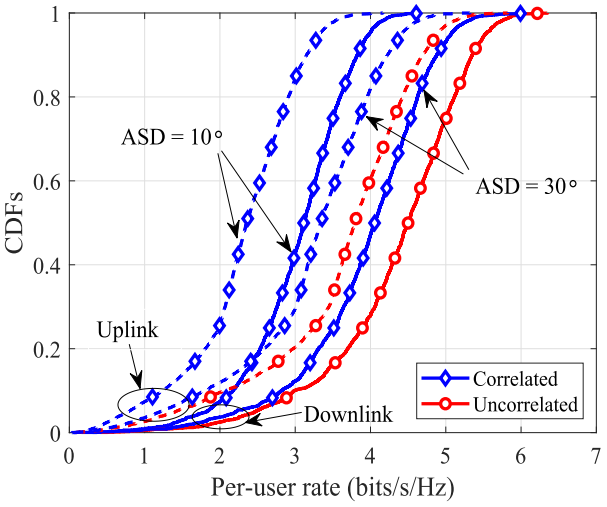

FIGURE 6. The CDFs of the achievable per-user rate for both the uplink and downlink with different ASD, with $M = 60$, $K = 10$, and $M = 10$.

system performance gain. As the Figs. 2 and 3, the spatial correlation will seriously reduce the system performance. For example, in order to achieve a constant value of 40 bits/s/Hz with $N = 20$, the required numbers of AP for "Uncorrelated" is 32, whilst it nearly 2.1 fold increased for the "Correlated" case. The results show that the impact of performance reduced due to channels correlation can be compensated by increasing the number of APs. The similar results for the downlink can be obtained from Fig. 5. As expected, the achievable rate for downlink is greater than the uplink case.

Next, in Fig. 6, we analyze the cumulative distribution functions (CDFs) of the achievable per-user rate for both the uplink and downlink with different ASD, with $M = 60$, $K = 10$, and $M = 10$. We consider the strong channels correlation "ASD = 10°" and the medium channels correlation "ASD = 30°". Obviously, the strong spatially correlated channels will cause severe space-selective fading.

With a view to verifying the effectiveness of the proposed allocation schemes for both uplink and downlink, in Figs. 7 and 8, the CDFs of the achievable per-user rate are plotted finally, with $M = 60, N = 10, K = 10$, and ASD = 10°. Note that each curve is generated by averaging 500 independent random channels realization. As we can see that the proposed power allocation algorithm for the uplink is capable of achieve the eminently improvement in terms of 95%-likely and median rate, which indicates that it can provides uniformly service for all users. For example, with GP algorithm, the 5%-outage rate of "Correlated" and "Uncorrelated" are 1.27 and 1.76, which are 1.55-fold and 1.18-fold higher than the case without algorithm. Similar results for the downlink can be obtained from Fig. 8, in which

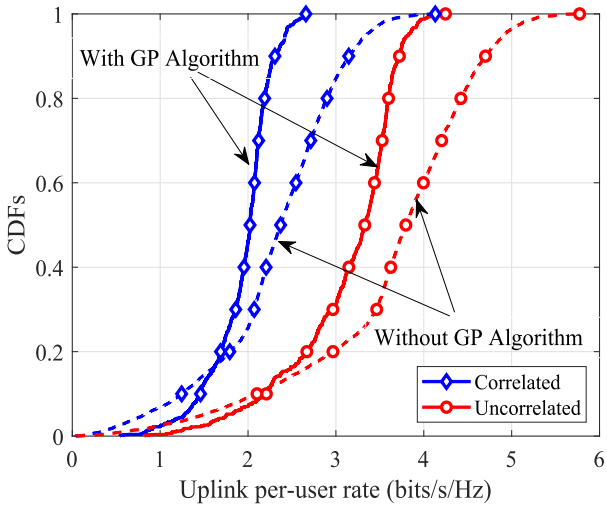

FIGURE 7. The CDFs of the achievable uplink per-user rate, with $M = 60, N = 10, K = 10$, and ASD = 10°.

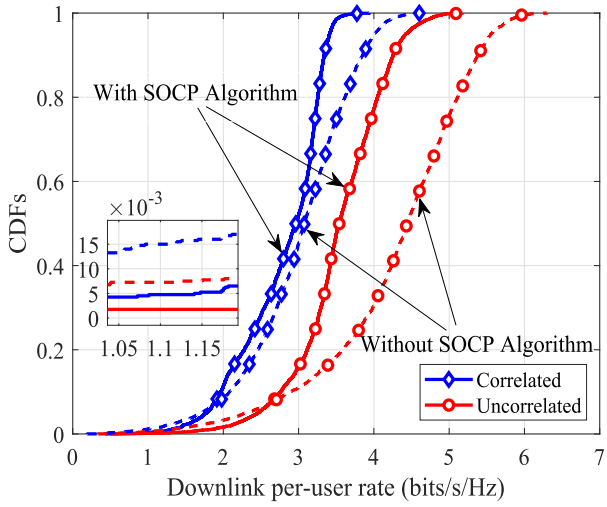

FIGURE 8. The CDFs of the achievable downlink per-user rate, with $M = 60, N = 10, K = 10$, and ASD = 10°.

the "Uncorrelated" is 1.2-fold and 1.3-fold for the scheme with and without SOCP algorithm.

VII. CONCLUSION

We have explored the spatially correlated Rayleigh fading for cell-free massive MIMO systems. With the low-complexity matched filter and conjugate beamforming, we derived the closed-form rigorous approximate expressions for both uplink and downlink, as well as the asymptotic performance analysis for infinite antenna array as well. The results show that channel correlation has a great deteriorating effect on the system performance. Finally, to provide uniformly good service to all geometrically distributed users, the max-min fairness power allocation strategies were proposed. We proved that the max-min fairness schemes for uplink and downlink can be effectively reformulated as GP and SOCP, respectively.

APPENDIXES

APPENDIX A
PROOF OF LEMMA 1

From (5), $\breve{\mathbf{y}}_{mk,\mathrm{p}}$ can be recast as

$$\breve{\mathbf{y}}_{mk,\mathrm{p}} = \underbrace{\sqrt{\tau\rho_{\mathrm{p}}}\mathbf{g}_{mk}}_{\text{desired channel}} + \underbrace{\sqrt{\tau\rho_{\mathrm{p}}}\sum_{k'\in\mathcal{P}_k\setminus\{k\}}\mathbf{g}_{mk'}}_{\text{interference channel}} + \underbrace{\mathbf{N}_{m,\mathrm{p}}\boldsymbol{\varphi}_k}_{\text{thermal noise}}. \tag{60}$$

Owing to the fact that $\mathbf{g}_{mk'} \sim \mathcal{N}_{\mathbb{C}}(\mathbf{0}, \mathbf{R}_{mk'})$, $\mathbf{N}_{m,\mathrm{p}}\boldsymbol{\varphi}_k \sim \mathcal{N}_{\mathbb{C}}(\mathbf{0}, \mathbf{I}_N)$, and by virtue of standard MMSE channel estimation technique [22], the estimated channel $\hat{\mathbf{g}}_{mk}$ can be given as

$$\begin{aligned}\hat{\mathbf{g}}_{mk} &= \frac{\sqrt{\tau\rho_{\mathrm{p}}}\mathbf{R}_{mk}}{\tau\rho_{\mathrm{p}}\mathbf{R}_{mk} + \tau\rho_{\mathrm{p}}\sum\limits_{k'\in\mathcal{P}_k\setminus\{k\}}\mathbf{R}_{mk'} + \mathbf{I}_N}\breve{\mathbf{y}}_{mk,\mathrm{p}} \\ &= \sqrt{\tau\rho_{\mathrm{p}}}\mathbf{R}_{mk}\boldsymbol{\Xi}_{mk}\breve{\mathbf{y}}_{mk,\mathrm{p}},\end{aligned} \tag{61}$$

where $\boldsymbol{\Xi}_{mk}$ is defined as (7). As a result, the level of the covariance matrix $\hat{\mathbf{g}}_{mk}$ can be measured by

$$\begin{aligned}&\mathbb{E}\left\{\hat{\mathbf{g}}_{mk}\hat{\mathbf{g}}_{mk}^H\right\} \\ &= \tau\rho_{\mathrm{p}}\mathbb{E}\left\{\mathbf{R}_{mk}\boldsymbol{\Xi}_{mk}\breve{\mathbf{y}}_{mk,\mathrm{p}}\breve{\mathbf{y}}_{mk,\mathrm{p}}^H\boldsymbol{\Xi}_{mk}\mathbf{R}_{mk}\right\} \\ &= \tau\rho_{\mathrm{p}}\mathbf{R}_{mk}\boldsymbol{\Xi}_{mk}\mathbf{R}_{mk}.\end{aligned} \tag{62}$$

Since $\tilde{\mathbf{g}}_{mk}$ and $\hat{\mathbf{g}}_{mk}$ are uncorrelated under the MMSE principle, then the covariance matrix of $\tilde{\mathbf{g}}_{mk}$ equals to

$$\begin{aligned}\mathbb{E}\left\{\tilde{\mathbf{g}}_{mk}\tilde{\mathbf{g}}_{mk}^H\right\} &= \mathbb{E}\left\{\left(\mathbf{g}_{mk} - \hat{\mathbf{g}}_{mk}\right)\left(\mathbf{g}_{mk} - \hat{\mathbf{g}}_{mk}\right)^H\right\} \\ &= \mathbb{E}\left\{\mathbf{g}_{mk}\mathbf{g}_{mk}^H\right\} - \mathbb{E}\left\{\hat{\mathbf{g}}_{mk}\hat{\mathbf{g}}_{mk}^H\right\} \\ &= \mathbf{R}_{mk} - \tau\rho_{\mathrm{p}}\mathbf{R}_{mk}\boldsymbol{\Xi}_{mk}\mathbf{R}_{mk}.\end{aligned} \tag{64}$$

Consequently, the results in lemma 1 can be achieved.

APPENDIX B
PROOF OF THEOREM 1

Before providing the detailed mathematical analysis in regard to deriving the achievable uplink rate (20), we first establish some mathematical motivations and preliminaries, which are instrumental for deriving the desired lower bound and evaluating the system performance.

Lemma 3: For the spatially correlated Rayleigh fading channels, the expectation of the inner product of $\hat{\mathbf{g}}_{mk}$ and $\mathbf{g}_{mk'}, \forall m$ is given by

$$\mathbb{E}\left\{\hat{\mathbf{g}}_{mk}^H\mathbf{g}_{mk'}\right\} = \begin{cases}0, & \forall k' \notin \mathcal{P}_k \\ \tau\rho_{\mathrm{p}}\mathrm{tr}\left(\mathbf{R}_{mk'}\mathbf{R}_{mk}\boldsymbol{\Xi}_{mk}\right), & \forall k' \in \mathcal{P}_k.\end{cases} \tag{65}$$

Proof: With the fact that $\mathbb{E}\left\{\hat{\mathbf{g}}_{mk}^H\mathbf{g}_{mk'}\right\} = \mathbb{E}\left\{\hat{\mathbf{g}}_{mk}^H\hat{\mathbf{g}}_{mk'}\right\}$, therefore, $\mathbb{E}\left\{\hat{\mathbf{g}}_{mk}^H\mathbf{g}_{mk'}\right\}$ can be depomposed into the following two cases:

1) For $\forall k' \notin \mathcal{P}_k$,
We can easily obtain $\mathbb{E}\left\{\hat{\mathbf{g}}_{mk}^H \mathbf{g}_{mk'}\right\} = 0$, since $\hat{\mathbf{g}}_{mk}$ is uncorrelated with $\mathbf{g}_{mk'}$ and both have zero mean.
2) For $\forall k' \in \mathcal{P}_k$,
Substituting (6) into $\mathbb{E}\left\{\hat{\mathbf{g}}_{mk}^H \mathbf{g}_{mk'}\right\}$ leads to

$$\begin{aligned}&\mathbb{E}\left\{\hat{\mathbf{g}}_{mk}^H \hat{\mathbf{g}}_{mk'}\right\}\\ &\overset{(a)}{=} \tau\rho_{\mathrm{p}}\mathrm{tr}\left(\mathbb{E}\left\{\mathbf{R}_{mk'}\boldsymbol{\Xi}_{mk}\breve{\mathbf{y}}_{mk,\mathrm{p}}\breve{\mathbf{y}}_{mk,\mathrm{p}}^H\boldsymbol{\Xi}_{mk}\mathbf{R}_{mk}\right\}\right)\\ &= \tau\rho_{\mathrm{p}}\mathrm{tr}\left(\mathbf{R}_{mk'}\mathbf{R}_{mk}\boldsymbol{\Xi}_{mk}\right), \end{aligned} \tag{66}$$

where (a) follows the fact $\boldsymbol{\Xi}_{mk} = \boldsymbol{\Xi}_{mk'}$ and $\breve{\mathbf{y}}_{mk,\mathrm{p}} = \breve{\mathbf{y}}_{mk',\mathrm{p}}$.

Lemma 4: The expectation of the norm-square of $\hat{\mathbf{g}}_{mk}$ and $\mathbf{g}_{mk'}$, $\forall m$ can be given as (63), as shown at the bottom of this page.

Proof:

1) For $\forall k' \notin \mathcal{P}_k$,

$$\begin{aligned}\mathbb{E}\left\{\left|\hat{\mathbf{g}}_{mk}^H \mathbf{g}_{mk'}\right|^2\right\} &= \mathbb{E}\left\{\hat{\mathbf{g}}_{mk}^H \mathbf{g}_{mk'}\mathbf{g}_{mk'}^H \hat{\mathbf{g}}_{mk}\right\}\\ &= \mathrm{tr}\left(\mathbb{E}\left\{\mathbf{g}_{mk'}\mathbf{g}_{mk'}^H \hat{\mathbf{g}}_{mk}\hat{\mathbf{g}}_{mk}^H\right\}\right)\\ &= \tau\rho_{\mathrm{p}}\cdot\mathrm{tr}\left(\mathbf{R}_{mk'}\mathbf{R}_{mk}\boldsymbol{\Xi}_{mk}\mathbf{R}_{mk}\right). \end{aligned} \tag{67}$$

2) For $\forall k' \in \mathcal{P}_k$,

$$\begin{aligned}&\mathbb{E}\left\{\left|\hat{\mathbf{g}}_{mk}^H \mathbf{g}_{mk'}\right|^2\right\}\\ &= \mathbb{E}\left\{\hat{\mathbf{g}}_{mk}^H\left(\hat{\mathbf{g}}_{mk'} + \tilde{\mathbf{g}}_{mk'}\right)\left(\hat{\mathbf{g}}_{mk'}^H + \tilde{\mathbf{g}}_{mk'}^H\right)\hat{\mathbf{g}}_{mk}\right\}\\ &= \mathbb{E}\left\{\hat{\mathbf{g}}_{mk}^H \hat{\mathbf{g}}_{mk'}\hat{\mathbf{g}}_{mk'}^H \hat{\mathbf{g}}_{mk}\right\} + \mathbb{E}\left\{\hat{\mathbf{g}}_{mk}^H \tilde{\mathbf{g}}_{mk'}\tilde{\mathbf{g}}_{mk'}^H \hat{\mathbf{g}}_{mk}\right\}. \end{aligned} \tag{68}$$

Since $\forall k' \in \mathcal{P}_k$, therefore we have $\breve{\mathbf{y}}_{mk,\mathrm{p}} = \breve{\mathbf{y}}_{mk',\mathrm{p}}$ and $\boldsymbol{\Xi}_{mk} = \boldsymbol{\Xi}_{mk'}$. For the first term $\mathbb{E}\left\{\hat{\mathbf{g}}_{mk}^H \hat{\mathbf{g}}_{mk'}\hat{\mathbf{g}}_{mk'}^H \hat{\mathbf{g}}_{mk}\right\}$, we have

$$\mathbb{E}\left\{\breve{\mathbf{y}}_{mk,\mathrm{p}}\breve{\mathbf{y}}_{mk,\mathrm{p}}^H\right\} = \tau\rho_{\mathrm{p}}\sum_{k'\in\mathcal{P}_k}\mathbf{R}_{mk'} + \mathbf{I}_N = (\boldsymbol{\Xi}_{mk})^{-1}. \tag{69}$$

Therefore, we can obtain

$$\breve{\mathbf{y}}_{mk,\mathrm{p}} \sim \mathcal{N}_{\mathbb{C}}\left(\mathbf{0},\ (\boldsymbol{\Xi}_{mk})^{-1}\right). \tag{70}$$

From (6), the first term $\mathbb{E}\left\{\hat{\mathbf{g}}_{mk}^H \hat{\mathbf{g}}_{mk'}\hat{\mathbf{g}}_{mk'}^H \hat{\mathbf{g}}_{mk}\right\}$ can be rewritten as

$$\begin{aligned}&\mathbb{E}\left\{\hat{\mathbf{g}}_{mk}^H \hat{\mathbf{g}}_{mk'}\hat{\mathbf{g}}_{mk'}^H \hat{\mathbf{g}}_{mk}\right\}\\ &= \mathbb{E}\left\{\tau^2\rho_{\mathrm{p}}^2\cdot\left|\left(\mathbf{R}_{mk'}\boldsymbol{\Xi}_{mk}\breve{\mathbf{y}}_{mk,\mathrm{p}}\right)^H\mathbf{R}_{mk}\boldsymbol{\Xi}_{mk}\breve{\mathbf{y}}_{mk,\mathrm{p}}\right|^2\right\}\\ &= \tau^2\rho_{\mathrm{p}}^2\cdot\mathbb{E}\left\{\left|\breve{\mathbf{y}}_{mk,\mathrm{p}}^H\boldsymbol{\Xi}_{mk}\mathbf{R}_{mk'}\mathbf{R}_{mk}\boldsymbol{\Xi}_{mk}\breve{\mathbf{y}}_{mk,\mathrm{p}}\right|^2\right\}. \end{aligned} \tag{71}$$

With the random matrix theory and the fact that $\|\mathbf{A}\|^2 = \mathrm{tr}\left(\mathbf{A}\mathbf{A}^H\right)$, we have the following result shown as [20]

$$\mathbb{E}\left\{\left|\mathbf{a}^H\mathbf{B}\mathbf{a}\right|^2\right\} = |\mathrm{tr}(\mathbf{B}\mathbf{A})|^2 + \mathrm{tr}\left(\mathbf{B}\mathbf{A}\mathbf{B}^H\mathbf{A}\right), \tag{72}$$

where the vector $\mathbf{a} \sim \mathcal{N}_{\mathbb{C}}(\mathbf{0}, \mathbf{A})$ with covariance matrix $\mathbf{A} \in \mathbb{C}^{N\times N}$ and any diagonalizable matrix $\mathbf{B} \in \mathbb{C}^{N\times N}$. By exploiting the above property, we can obtain the following results. Straight-forward computations $\mathbb{E}\left\{\hat{\mathbf{g}}_{mk}^H \hat{\mathbf{g}}_{mk'}\hat{\mathbf{g}}_{mk'}^H \hat{\mathbf{g}}_{mk}\right\}$ can be yield to

$$\begin{aligned}&\mathbb{E}\left\{\hat{\mathbf{g}}_{mk}^H \hat{\mathbf{g}}_{mk'}\hat{\mathbf{g}}_{mk'}^H \hat{\mathbf{g}}_{mk}\right\}\\ &= \tau^2\rho_{\mathrm{p}}^2\cdot\left(\left|\mathrm{tr}\left(\boldsymbol{\Xi}_{mk}\mathbf{R}_{mk'}\mathbf{R}_{mk}\boldsymbol{\Xi}_{mk}\boldsymbol{\Xi}_{mk}^{-1}\right)\right|^2\right.\\ &\quad\left.+\mathrm{tr}\left(\boldsymbol{\Xi}_{mk}\mathbf{R}_{mk'}\mathbf{R}_{mk}\boldsymbol{\Xi}_{mk}\boldsymbol{\Xi}_{mk}^{-1}\boldsymbol{\Xi}_{mk}\mathbf{R}_{mk}\mathbf{R}_{mk'}\boldsymbol{\Xi}_{mk}\boldsymbol{\Xi}_{mk}^{-1}\right)\right)\\ &= \tau^2\rho_{\mathrm{p}}^2\cdot\left(\left|\mathrm{tr}\left(\boldsymbol{\Xi}_{mk}\mathbf{R}_{mk'}\mathbf{R}_{mk}\right)\right|^2\right.\\ &\quad\left.+\ \mathrm{tr}\left(\boldsymbol{\Xi}_{mk}\mathbf{R}_{mk'}\mathbf{R}_{mk}\boldsymbol{\Xi}_{mk}\mathbf{R}_{mk}\mathbf{R}_{mk'}\right)\right)\\ &\overset{(b)}{=} \tau^2\rho_{\mathrm{p}}^2\cdot\left|\mathrm{tr}\left(\boldsymbol{\Xi}_{mk}\mathbf{R}_{mk'}\mathbf{R}_{mk}\right)\right|^2\\ &\quad+\tau\rho_{\mathrm{p}}\cdot\mathrm{tr}\left(\left(\mathbf{R}_{mk'}-\mathbf{C}_{mk'}\right)\mathbf{R}_{mk}\boldsymbol{\Xi}_{mk}\mathbf{R}_{mk}\right)\\ &= \tau^2\rho_{\mathrm{p}}^2\cdot\left|\mathrm{tr}\left(\mathbf{R}_{mk'}\mathbf{R}_{mk}\boldsymbol{\Xi}_{mk}\right)\right|^2\\ &\quad+\tau\rho_{\mathrm{p}}\cdot\mathrm{tr}\left(\left(\mathbf{R}_{mk'}-\mathbf{C}_{mk'}\right)\mathbf{R}_{mk}\boldsymbol{\Xi}_{mk}\mathbf{R}_{mk}\right), \end{aligned} \tag{74}$$

where (b) follows $\mathrm{tr}(\mathbf{ABC}) = \mathrm{tr}(\mathbf{CAB}) = \mathrm{tr}(\mathbf{BCA})$.

Consequently, for the second term $\mathbb{E}\left\{\hat{\mathbf{g}}_{mk}^H \tilde{\mathbf{g}}_{mk'}\tilde{\mathbf{g}}_{mk'}^H \hat{\mathbf{g}}_{mk}\right\}$, we have

$$\begin{aligned}&\mathbb{E}\left\{\hat{\mathbf{g}}_{mk}^H \tilde{\mathbf{g}}_{mk'}\tilde{\mathbf{g}}_{mk'}^H \hat{\mathbf{g}}_{mk}\right\}\\ &= \mathrm{tr}\left(\mathbb{E}\left\{\tilde{\mathbf{g}}_{mk'}\tilde{\mathbf{g}}_{mk'}^H\right\}\cdot\mathbb{E}\left\{\hat{\mathbf{g}}_{mk}\hat{\mathbf{g}}_{mk}^H\right\}\right)\\ &= \mathrm{tr}\left(\mathbf{C}_{mk'}\tau\rho_{\mathrm{p}}\mathbf{R}_{mk}\boldsymbol{\Xi}_{mk}\mathbf{R}_{mk}\right)\\ &= \tau\rho_{\mathrm{p}}\cdot\mathrm{tr}\left(\mathbf{C}_{mk'}\mathbf{R}_{mk}\boldsymbol{\Xi}_{mk}\mathbf{R}_{mk}\right). \end{aligned} \tag{75}$$

$$\mathbb{E}\left\{\left|\hat{\mathbf{g}}_{mk}^H \mathbf{g}_{mk'}\right|^2\right\} = \begin{cases}\tau\rho_{\mathrm{p}}\cdot\mathrm{tr}\left(\mathbf{R}_{mk'}\mathbf{R}_{mk}\boldsymbol{\Xi}_{mk}\mathbf{R}_{mk}\right), & k' \notin \mathcal{P}_k\\ \tau^2\rho_{\mathrm{p}}^2\cdot|\mathrm{tr}\left(\mathbf{R}_{mk'}\mathbf{R}_{mk}\boldsymbol{\Xi}_{mk}\right)|^2 + \tau\rho_{\mathrm{p}}\cdot\mathrm{tr}\left(\mathbf{R}_{mk'}\mathbf{R}_{mk}\boldsymbol{\Xi}_{mk}\mathbf{R}_{mk}\right), & k' \in \mathcal{P}_k\end{cases} \tag{63}$$

$$\mathbb{E}\left\{\left|\sum_{m=1}^{M}\hat{\mathbf{g}}_{mk}^H \mathbf{g}_{mk'}\right|^2\right\} = \begin{cases}\tau\rho_{\mathrm{p}}\sum\limits_{m=1}^{M}\mathrm{tr}\left(\mathbf{R}_{mk'}\left(\mathbf{Q}_{mk}\right)\right), & k' \notin \mathcal{P}_k\\ \tau^2\rho_{\mathrm{p}}^2\left(\sum\limits_{m=1}^{M}\mathrm{tr}\left(\mathbf{R}_{mk'}\mathbf{R}_{mk}\boldsymbol{\Xi}_{mk}\right)\right)^2 + \sum\limits_{m=1}^{M}\mathrm{tr}\left(\mathbf{R}_{mk'}\left(\mathbf{Q}_{mk}\right)\right), & k' \in \mathcal{P}_k\end{cases} \tag{73}$$

Combining (74) with (75), we can achieve

$$\mathbb{E}\left\{\left|\hat{\mathbf{g}}_{mk}^{H}\mathbf{g}_{mk'}\right|^{2}\right\}=\tau^{2}\rho_{\mathrm{p}}^{2}\cdot\left|\mathrm{tr}\left(\mathbf{R}_{mk'}\mathbf{R}_{mk}\boldsymbol{\Xi}_{mk}\right)\right|^{2}+\tau\rho_{\mathrm{p}}\mathrm{tr}\left(\mathbf{R}_{mk'}\mathbf{R}_{mk}\boldsymbol{\Xi}_{mk}\mathbf{R}_{mk}\right). \tag{76}$$

Through the above-described procedure, $\mathbb{E}\left\{\left\|\hat{\mathbf{g}}_{mk}\right\|^{4}\right\}$ can be given as

$$\mathbb{E}\left\{\left\|\hat{\mathbf{g}}_{mk}\right\|^{4}\right\}=\tau^{2}\rho_{\mathrm{p}}^{2}\left|\mathrm{tr}\left(\mathbf{R}_{mk}\mathbf{R}_{mk}\boldsymbol{\Xi}_{mk}\right)\right|^{2}+\tau\rho_{\mathrm{p}}\mathrm{tr}\left(\left(\mathbf{R}_{mk}-\mathbf{C}_{mk}\right)\mathbf{R}_{mk}\boldsymbol{\Xi}_{mk}\mathbf{R}_{mk}\right). \tag{77}$$

Therefore, we can complete the proof of the lemma 4.

Lemma 5: The expectation of the norm-square of the sum inner product of $\hat{\mathbf{g}}_{mk}$ and $\mathbf{g}_{mk'}$, $\forall m$ can be expressed as (73), as shown at the bottom of the previous page.

Proof: The term $\mathbb{E}\left\{\left|\sum_{m=1}^{M}\hat{\mathbf{g}}_{mk}^{H}\mathbf{g}_{mk'}\right|^{2}\right\}$ can be rewritten as

$$\mathbb{E}\left\{\left|\sum\nolimits_{m=1}^{M}\hat{\mathbf{g}}_{mk}^{H}\mathbf{g}_{mk'}\right|^{2}\right\}=\mathbb{E}\left\{\sum\nolimits_{m=1}^{M}\sum\nolimits_{n=1}^{M}\hat{\mathbf{g}}_{mk}^{H}\mathbf{g}_{mk'}\mathbf{g}_{nk'}^{H}\hat{\mathbf{g}}_{nk}\right\}, \tag{78}$$

which can be decomposed into the following four cases:

1) For $n\neq m$ and $\forall k'\notin\mathcal{P}_{k}$,

$$\mathbb{E}\left\{\sum_{m=1}^{M}\sum_{n\neq m}^{M}\hat{\mathbf{g}}_{mk}^{H}\mathbf{g}_{mk'}\mathbf{g}_{nk'}^{H}\hat{\mathbf{g}}_{nk}\right\}=\sum_{m=1}^{M}\sum_{n\neq m}^{M}\mathbb{E}\left\{\hat{\mathbf{g}}_{mk}^{H}\mathbf{g}_{mk'}\mathbf{g}_{nk'}^{H}\hat{\mathbf{g}}_{nk}\right\}\overset{(c)}{=}0, \tag{79}$$

where (c) is owing to the fact that $\hat{\mathbf{g}}_{mk}$ is uncorrelated with $\mathbf{g}_{nk'}$ and both have zero mean.

2) For $n\neq m$ and $\forall k'\in\mathcal{P}_{k}$,

$$\begin{aligned}&\mathbb{E}\left\{\sum_{m=1}^{M}\sum_{n\neq m}^{M}\hat{\mathbf{g}}_{mk}^{H}\mathbf{g}_{mk'}\mathbf{g}_{nk'}^{H}\hat{\mathbf{g}}_{nk}\right\}\\&=\sum_{m=1}^{M}\sum_{n\neq m}^{M}\mathbb{E}\left\{\hat{\mathbf{g}}_{mk}^{H}\mathbf{g}_{mk'}\right\}\cdot\mathbb{E}\left\{\mathbf{g}_{nk'}^{H}\hat{\mathbf{g}}_{nk}\right\}\\&=\tau^{2}\rho_{\mathrm{p}}^{2}\sum_{m=1}^{M}\sum_{n\neq m}^{M}\mathrm{tr}\left(\mathbf{R}_{mk'}\mathbf{R}_{mk}\boldsymbol{\Xi}_{mk}\right)\cdot\mathrm{tr}\left(\boldsymbol{\Xi}_{nk}\mathbf{R}_{nk}\mathbf{R}_{nk'}\right),\end{aligned} \tag{80}$$

3) For $n=m$, and $\forall k'\in\mathcal{P}_{k}$,

$$\begin{aligned}&\sum_{m=1}^{M}\mathbb{E}\left\{\hat{\mathbf{g}}_{mk}^{H}\mathbf{g}_{mk'}\mathbf{g}_{mk'}^{H}\hat{\mathbf{g}}_{mk}\right\}\\&=\sum_{m=1}^{M}\mathbb{E}\left\{\left|\hat{\mathbf{g}}_{mk}^{H}\mathbf{g}_{mk'}\right|^{2}\right\}\\&=\sum_{m=1}^{M}\left(\tau^{2}\rho_{\mathrm{p}}^{2}\left|\mathrm{tr}\left(\mathbf{R}_{mk'}\mathbf{R}_{mk}\boldsymbol{\Xi}_{mk}\right)\right|^{2}+\mathrm{tr}\left(\mathbf{R}_{mk'}\left(\mathbf{Q}_{mk}\right)\right)\right).\end{aligned} \tag{81}$$

4) For $n=m$, and $\forall k'\notin\mathcal{P}_{k}$,

$$\begin{aligned}&\sum_{m=1}^{M}\mathbb{E}\left\{\hat{\mathbf{g}}_{mk}^{H}\mathbf{g}_{mk'}\mathbf{g}_{mk'}^{H}\hat{\mathbf{g}}_{mk}\right\}\\&=\sum_{m=1}^{M}\mathrm{tr}\left(\mathbb{E}\left\{\mathbf{g}_{mk'}\mathbf{g}_{mk'}^{H}\right\}\cdot\mathbb{E}\left\{\hat{\mathbf{g}}_{mk}\hat{\mathbf{g}}_{mk}^{H}\right\}\right)\\&=\sum_{m=1}^{M}\mathrm{tr}\left(\mathbf{R}_{mk'}\left(\mathbf{Q}_{mk}\right)\right).\end{aligned} \tag{82}$$

With the (79)-(82), we complete the proof of lemma 5.

Based on the above presented lemmas, now we calculate A_k, B_{1k}, B_{2k}, and B_{3k}.

1) Compute A_k,

$$\begin{aligned}A_{k}&=\rho_{\mathrm{u}}\eta_{k}\left|\sum_{m=1}^{M}\mathbb{E}\left\{\hat{\mathbf{g}}_{mk}^{H}\mathbf{g}_{mk}\right\}\right|^{2}\\&=\rho_{\mathrm{u}}\eta_{k}\left|\sum_{m=1}^{M}\mathbb{E}\left\{\hat{\mathbf{g}}_{mk}^{H}\left(\hat{\mathbf{g}}_{mk}+\tilde{\mathbf{g}}_{mk}\right)\right\}\right|^{2}\\&=\rho_{\mathrm{u}}\eta_{k}\left|\sum_{m=1}^{M}\mathrm{tr}\left(\mathbf{Q}_{mk}\right)\right|^{2}.\end{aligned} \tag{83}$$

2) Compute B_{1k},

$$\begin{aligned}B_{1k}&=\rho_{\mathrm{u}}\eta_{k}\mathbb{E}\left\{\left|\sum_{m=1}^{M}\hat{\mathbf{g}}_{mk}^{H}\mathbf{g}_{mk}-\mathbb{E}\left\{\sum_{m=1}^{M}\hat{\mathbf{g}}_{mk}^{H}\mathbf{g}_{mk}\right\}\right|^{2}\right\}\\&=\rho_{\mathrm{u}}\eta_{k}\mathbb{E}\left\{\left|\sum_{m=1}^{M}\hat{\mathbf{g}}_{mk}^{H}\mathbf{g}_{mk}\right|^{2}-\left|\mathbb{E}\left\{\sum_{m=1}^{M}\hat{\mathbf{g}}_{mk}^{H}\mathbf{g}_{mk}\right\}\right|^{2}\right\}\\&\overset{(d)}{=}\rho_{\mathrm{u}}\eta_{k}\mathbb{E}\left\{\tau^{2}\rho_{\mathrm{p}}^{2}\left(\sum_{m=1}^{M}\mathrm{tr}\left(\mathbf{R}_{mk}\mathbf{R}_{mk}\boldsymbol{\Xi}_{mk}\right)\right)^{2}+\tau\rho_{\mathrm{p}}\sum_{m=1}^{M}\mathrm{tr}\left(\mathbf{R}_{mk}\mathbf{R}_{mk}\boldsymbol{\Xi}_{mk}\mathbf{R}_{mk}\right)-\tau^{2}\rho_{\mathrm{p}}^{2}\left(\sum_{m=1}^{M}\mathrm{tr}\left(\mathbf{R}_{mk}\mathbf{R}_{mk}\boldsymbol{\Xi}_{mk}\right)\right)^{2}\right\}\\&=\rho_{\mathrm{u}}\eta_{k}\sum_{m=1}^{M}\mathrm{tr}\left(\mathbf{R}_{mk}\left(\mathbf{Q}_{mk}\right)\right),\end{aligned} \tag{84}$$

where (d) is obtained from lemma 3.

3) Compute B_{2k},

$$B_{2k}=\rho_{\mathrm{u}}\sum_{k'\neq k}^{K}\eta_{k'}\mathbb{E}\left\{\left|\sum_{m=1}^{M}\hat{\mathbf{g}}_{mk}^{H}\mathbf{g}_{mk'}\right|^{2}\right\}\overset{(e)}{=}\rho_{\mathrm{u}}\sum_{k'\in\mathcal{P}_{k}\setminus\{k\}}\eta_{k'}\left(\tau^{2}\rho_{\mathrm{p}}^{2}\left|\sum_{m=1}^{M}\mathrm{tr}\left(\mathbf{R}_{mk'}\mathbf{R}_{mk}\boldsymbol{\Xi}_{mk}\right)\right|^{2}\right.$$

$$+\sum_{m=1}^{M}\mathrm{tr}\left(\mathbf{R}_{mk'}\left(\mathbf{Q}_{mk}\right)\right)\Bigg)$$
$$+\rho_{\mathrm{u}}\sum_{k'\notin\mathcal{P}_k}\eta_{k'}\sum_{m=1}^{M}\mathrm{tr}\left(\mathbf{R}_{mk'}\left(\mathbf{Q}_{mk}\right)\right)$$
$$=\tau^2\rho_{\mathrm{p}}^2\rho_{\mathrm{u}}\sum_{k'\in\mathcal{P}_k\setminus\{k\}}\eta_{k'}\left|\sum_{m=1}^{M}\mathrm{tr}\left(\mathbf{R}_{mk'}\mathbf{R}_{mk}\boldsymbol{\Xi}_{mk}\right)\right|^2$$
$$+\rho_{\mathrm{u}}\sum_{k'\neq k}^{K}\eta_{k'}\sum_{m=1}^{M}\mathrm{tr}\left(\mathbf{R}_{mk'}\left(\mathbf{Q}_{mk}\right)\right), \tag{85}$$

where (e) is derived from lemmas 4 and 5.

4) Compute B_{3k},

$$\begin{aligned}B_{3k}&=\mathbb{E}\left\{\left|\sum_{m=1}^{M}\hat{\mathbf{g}}_{mk}^H\mathbf{n}_{m,\mathrm{u}}\right|^2\right\}\\&=\mathbb{E}\left\{\sum_{m=1}^{M}\hat{\mathbf{g}}_{mk}^H\cdot\mathbb{E}\left\{\mathbf{n}_{m,\mathrm{u}}\mathbf{n}_{m,\mathrm{u}}^H\right\}\cdot\hat{\mathbf{g}}_{mk}\right\}\\&=\sum_{m=1}^{M}\mathrm{tr}\left(\mathbf{Q}_{mk}\right).\end{aligned} \tag{86}$$

Substituting (83)-(86) into (20), the desired results can be arrived after some simple mathematical derivations.

APPENDIX C
PROOF OF THEOREM 3

With the results presented in (13), we have

$$\begin{aligned}r_{k,\mathrm{u}}=&\sqrt{\rho_{\mathrm{u}}}\sum_{m=1}^{M}\sqrt{\eta_k}\hat{\mathbf{g}}_{mk}^H\mathbf{g}_{mk}q_k\\&+\sqrt{\rho_{\mathrm{u}}}\sum_{k'\neq k}^{K}\sum_{m=1}^{M}\sqrt{\eta_{k'}}\hat{\mathbf{g}}_{mk}^H\mathbf{g}_{mk'}q_{k'}+\sum_{m=1}^{M}\hat{\mathbf{g}}_{mk}^H\mathbf{n}_{m,\mathrm{u}}.\end{aligned} \tag{87}$$

Then, with (6), the $\hat{\mathbf{g}}_{mk}^H\mathbf{g}_{mk'}$ can be expressed as

$$\begin{aligned}\hat{\mathbf{g}}_{mk}^H\mathbf{g}_{mk'}=&\,\tau\rho_{\mathrm{p}}\mathbf{R}_{mk}\boldsymbol{\Xi}_{mk}\mathbf{g}_{mk'}^H\mathbf{g}_{mk'}\boldsymbol{\varphi}_{k'}^H\boldsymbol{\varphi}_k\\&+\tau\rho_{\mathrm{p}}\mathbf{R}_{mk}\boldsymbol{\Xi}_{mk}\sum_{k''\in\mathcal{P}_k\setminus\{k''\}}\mathbf{g}_{mk''}^H\mathbf{g}_{mk'}\\&+\boldsymbol{\varphi}_{k'}^H\mathbf{N}_{m,\mathrm{p}}^H\mathbf{g}_{mk'}.\end{aligned} \tag{88}$$

Therefore, we have

$$\begin{aligned}&\frac{1}{M}\sqrt{\rho_{\mathrm{u}}\eta_k}\sum_{m=1}^{M}\hat{\mathbf{g}}_{mk}^H\mathbf{g}_{mk}\\&\quad-\frac{\tau\rho_{\mathrm{p}}}{M}\sqrt{\rho_{\mathrm{u}}\eta_k}\sum_{m=1}^{M}\mathrm{tr}\left(\mathbf{R}_{mk}\boldsymbol{\Xi}_{mk}\mathbf{R}_{mk}\right)\xrightarrow[M\to\infty]{\text{a.s.}}0,\end{aligned} \tag{89}$$

where "$\xrightarrow[M\to\infty]{\text{a.s.}}0$" denotes almost sure convergence.

APPENDIX D
PROOF OF THEOREM 5

Proof: Due to the fact that the form of the SINR constraint in (29) is not a polynomial functions, therefore, we can convert into the following polynomial form as (90), as shown at the bottom of this page, where Ψ is given by

$$\Psi=\rho_{\mathrm{u}}\sum_{k'\neq k}^{K}\eta_{k'}\sum_{m=1}^{M}\mathrm{tr}\left(\mathbf{R}_{mk'}\left(\mathbf{Q}_{mk}\right)\right)+\sum_{m=1}^{M}\mathrm{tr}\left(\mathbf{Q}_{mk}\right). \tag{91}$$

Thus, (90) can be written as follows

$$\eta_k^{-1}\left(\sum_{m=1}^{M}a_{mk}\eta_k+\left(\tau^2\rho_{\mathrm{p}}^2b_{kk'}+c_{kk'}\right)\eta_{k'}+\frac{d_k}{\rho_{\mathrm{u}}}\right)\leq\frac{1}{t}, \tag{92}$$

where a_{mk}, $b_{kk'}$, $c_{kk'}$ and d_k can be respectively denoted as

$$a_{mk}=\frac{\mathrm{tr}\left(\mathbf{R}_{mk}\left(\mathbf{Q}_{mk}\right)\right)}{\left(\mathrm{tr}\left(\mathbf{Q}_{mk}\right)\right)^2}, \tag{93}$$

$$b_{kk'}=\frac{\sum\limits_{k'\in\mathcal{P}_k\setminus\{k\}}\left|\sum\limits_{m=1}^{M}\mathrm{tr}\left(\mathbf{R}_{mk'}\mathbf{R}_{mk}\boldsymbol{\Xi}_{mk}\right)\right|^2}{\left(\sum\limits_{m=1}^{M}\mathrm{tr}\left(\mathbf{Q}_{mk}\right)\right)^2}, \tag{94}$$

$$c_{kk'}=\frac{\sum\limits_{k'\neq k}^{K}\sum\limits_{m=1}^{M}\mathrm{tr}\left(\mathbf{R}_{mk'}\left(\mathbf{Q}_{mk}\right)\right)}{\left(\sum\limits_{m=1}^{M}\mathrm{tr}\left(\mathbf{Q}_{mk}\right)\right)^2}, \tag{95}$$

$$d_k=\frac{\sum\limits_{m=1}^{M}\mathrm{tr}\left(\mathbf{Q}_{mk}\right)}{\rho_{\mathrm{u}}\left(\sum\limits_{m=1}^{M}\mathrm{tr}\left(\mathbf{Q}_{mk}\right)\right)^2}. \tag{96}$$

It is shown that the left-hand side of (92) is a polynomial function. Therefore, problem P_2 is a standard GP.

$$\frac{\rho_{\mathrm{u}}\eta_k\sum\limits_{m=1}^{M}\mathrm{tr}\left(\mathbf{R}_{mk}\left(\mathbf{Q}_{mk}\right)\right)+\tau^2\rho_{\mathrm{p}}^2\rho_{\mathrm{u}}\sum\limits_{k'\in\mathcal{P}_k\setminus\{k\}}\eta_{k'}\left|\sum\limits_{m=1}^{M}\mathrm{tr}\left(\mathbf{R}_{mk'}\mathbf{R}_{mk}\boldsymbol{\Xi}_{mk}\right)\right|^2+\Psi}{\rho_{\mathrm{u}}\eta_k\left(\sum\limits_{m=1}^{M}\mathrm{tr}\left(\mathbf{Q}_{mk}\right)\right)^2}\leq\frac{1}{t} \tag{90}$$

APPENDIX E
PROOF OF THEOREM 6

Define the set of variables in P_4 as $\mathcal{S} = \{\bar{\boldsymbol{\xi}}_k, u_{k'k}, v_{k'k}\}$, and the objective function as

$$h(\mathcal{S}) = \min_{\forall k} \frac{\left|\mathbf{a}_k^T \bar{\boldsymbol{\xi}}_k\right|^2}{\sum\limits_{k' \in \mathcal{P}_k \setminus \{k\}} u_{k'k}^2 + \sum\limits_{k'=1}^{K} v_{k'k}^2 + \frac{1}{\rho_\mathrm{d}}}. \tag{97}$$

Therefore, the super-level of $h(\mathcal{S})$ belongs to $\mathcal{S}$, for any $t \in \mathbb{R}_+$, can be given as

$$\begin{aligned} &Q(h,t) \\ &= \{\mathcal{S} : h(\mathcal{S}) \geq t\} \\ &= \left\{ \mathcal{S} : \min_{\forall k} \frac{\left|\mathbf{a}_k^T \bar{\boldsymbol{\xi}}_k\right|^2}{\sum\limits_{k' \in \mathcal{P}_k \setminus \{k\}} u_{k'k}^2 + \sum\limits_{k'=1}^{K} v_{k'k}^2 + \frac{1}{\rho_\mathrm{d}}} \geq t \right\} \\ &= \left\{ \mathcal{S} : \left\| \left[\mathbf{x}_{1k}^T \mathbf{I}_{+\mathcal{P}_k \setminus \{k\}}, \mathbf{x}_{2k}^T \mathbf{I}_K, \frac{1}{\sqrt{\rho_\mathrm{d}}} \right]^T \right\| \leq \frac{1}{\sqrt{t}} \mathbf{a}_k^T \bar{\boldsymbol{\xi}}_k, \forall k \right\}, \end{aligned} \tag{98}$$

where $\mathbf{I}_{+\mathcal{P}_k \setminus \{k\}}$ represents the matrix consisting of the k'-th, $(k' \in \mathcal{P}_k, k' \neq k)$ column of unit matrix $\mathbf{I}_K$ and $\mathbf{x}_{1k} = [u_{1k}, \ldots, u_{Kk}]^T$, $\mathbf{x}_{2k} = [v_{1k}, \ldots, v_{Kk}]^T$.

Since the super-level set $Q(h,t)$ can be written as an SOC, therefore, it is a convex set and $h(\mathcal{S})$ is quasi-concave. With the fact that the (59a) is a quasi-concave, the optimization problem is a quasi-concave and can be determined with the bisection method.

REFERENCES

[1] H. Q. Ngo, A. Ashikhmin, H. Yang, E. G. Larsson, and T. L. Marzetta, "Cell-free massive MIMO: Uniformly great service for everyone," in *Proc. IEEE 16th Int. Workshop Signal Process. Adv. Wireless Commun. (SPAWC)*, Jun. 2015, pp. 201–205.

[2] H. Q. Ngo, A. Ashikhmin, H. Yang, E. G. Larsson, and T. L. Marzetta, "Cell-free massive MIMO versus small cells," *IEEE Trans. Wireless Commun.*, vol. 16, no. 3, pp. 1834–1850, Mar. 2017.

[3] E. Nayebi, A. Ashikhmin, T. L. Marzetta, and H. Yang, "Cell-free massive MIMO systems," in *Proc. 49th Asilomar Conf. Signals, Syst. Comput.*, Nov. 2015, pp. 8757–8774.

[4] G. Interdonato, E. Björnson, H. Q. Ngo, P. Frenger, and E. G. Larsson, "Ubiquitous cell-free massive MIMO communications," *EURASIP J. Wireless Commun. Netw.*, vol. 2019, no. 1, pp. 1–13, Aug. 2019.

[5] M. Zhou, Y. Zhang, H. Cao, X. Qiao, and L. Yang, "Enhanced power allocation algorithms for uplink mixed ADCs massive MIMO systems," in *Proc. IEEE Global Commun. Conf. Workshops (GlobeCom Workshops)*, to be published.

[6] Y. Zhang, M. Zhou, H. Cao, L. Yang, and H. Zhu, "On the performance of cell-free massive MIMO with mixed-ADC under Rician fading channels," *IEEE Commun. Lett.*, vol. 24, no. 1, pp. 43–47, Jan. 2020.

[7] J. Zhang, S. Chen, Y. Lin, J. Zheng, B. Ai, and L. Hanzo, "Cell-free massive MIMO: A new next-generation paradigm," *IEEE Access*, vol. 7, pp. 99878–99888, Jul. 2019.

[8] Y. Zhang, M. Zhou, X. Qiao, H. Cao, and L. Yang, "On the performance of cell-free massive MIMO with low-resolution ADCs," *IEEE Access*, vol. 7, pp. 117968–117977, Aug. 2019.

[9] Z. Chen and E. Björnson, "Channel hardening and favorable propagation in cell-free massive MIMO with stochastic geometry," *IEEE Trans. Commun.*, vol. 66, no. 11, pp. 5205–5219, Nov. 2018.

[10] H. Q. Ngo, L.-N. Tran, T. Q. Duong, M. Matthaiou, and E. G. Larsson, "On the total energy efficiency of cell-free massive MIMO," *IEEE Trans. Green Commun. Netw.*, vol. 2, no. 1, pp. 25–39, Mar. 2018.

[11] E. Björnson, E. G. Larsson, and M. Debbah, "Massive MIMO for maximal spectral efficiency: How many users and pilots should be allocated?" *IEEE Trans. Wireless Commun.*, vol. 15, no. 2, pp. 1293–1308, Feb. 2016.

[12] G. Interdonato, M. Karlsson, E. Björnson, and E. G. Larsson, "Downlink spectral efficiency of cell-free massive MIMO with full-pilot zero-forcing," in *Proc. IEEE Global Conf. Signal Inf. Process. (GlobalSIP)*, Nov. 2018, pp. 1003–1007.

[13] Y. Li and G. A. Aruma Baduge, "NOMA-aided cell-free massive MIMO systems," *IEEE Wireless Commun. Lett.*, vol. 7, no. 6, pp. 950–953, Dec. 2018.

[14] Y. Zhang, H. Cao, M. Zhou, and L. Yang, "Spectral efficiency maximization for uplink cell-free massive MIMO-NOMA networks," in *Proc. IEEE Int. Conf. Commun. Workshops (ICC Workshops)*, May 2019, pp. 1–6.

[15] M. Bashar, K. Cumanan, A. G. Burr, H. Q. Ngo, L. Hanzo, and P. Xiao, "On the performance of cell-free massive MIMO relying on adaptive NOMA/OMA mode-switching," *IEEE Trans. Commun.*, vol. 68, no. 2, pp. 792–810, Feb. 2020, doi: 10.1109/TCOMM.2019.2952574.

[16] H. Tong and S. A. Zekavat, "Spatially correlated MIMO channel: Generation via virtual channel representation," *IEEE Commun. Lett.*, vol. 10, no. 5, pp. 332–334, May 2006.

[17] Q. Ding and Y. Lian, "Performance analysis of mixed-ADC massive MIMO systems over spatially correlated channels," *IEEE Access*, vol. 7, pp. 6842–6852, Dec. 2019.

[18] W. Xu, B. Wen, M. Lin, and X. Yu, "Energy-efficient power allocation scheme for distributed antenna system over spatially correlated Rayleigh channels," *IET Commun.*, vol. 12, no. 5, pp. 533–542, Mar. 2018.

[19] W. Fan, J. Zhang, E. Björnson, S. Chen, and Z. Zhong, "Performance analysis of cell-free massive MIMO over spatially correlated fading channels," in *Proc. IEEE Int. Conf. Commun. (ICC)*, May 2019, pp. 1–6.

[20] E. Björnson, J. Hoydis, and L. Sanguinetti, "Massive MIMO networks: Spectral, energy, and hardware efficiency," *Found. Trends Signal Process.*, vol. 11, nos. 3–4, pp. 154–655, 2017.

[21] X. Jia, P. Deng, L. Yang, and H. Zhu, "Spectrum and energy efficiencies for multiuser pairs massive MIMO systems with full-duplex Amplify-and-Forward relay," *IEEE Access*, vol. 3, pp. 1907–1918, Oct. 2015.

[22] F. Gao, T. Cui, and A. Nallanathan, "On channel estimation and optimal training design for amplify and forward relay networks," *IEEE Trans. Wireless Commun.*, vol. 7, no. 5, pp. 1907–1916, May 2008.

[23] H. Cramer, *Random Variables and Probability Distributions*. Cambridge, U.K.: Cambridge Univ. Press, 1970.

[24] N. T. Nghia, H. D. Tuan, T. Q. Duong, and H. V. Poor, "MIMO beamforming for secure and energy-efficient wireless communication," *IEEE Signal Process. Lett.*, vol. 24, no. 2, pp. 236–239, Feb. 2017.

MENG ZHOU received the M.S. degree from Northwest Normal University, Lanzhou, China, in 2018. He is currently pursuing the Ph.D. degree with the College of Communication and Information Engineering, Nanjing University of Posts and Telecommunications (NJUPT), Nanjing, China. His broad interests are in wireless communications, with a special interest of massive MIMO, physical layer security, as well as HetNets in 5G and beyond.

YAO ZHANG received the B.S. degree from the College of Computer Science and Technology, Qingdao University, China, in 2016. He is currently pursuing the Ph.D. degree with the Department of Communication and Information Engineering, Nanjing University of Posts and Telecommunications. His current research interests include massive (large-scale) MIMO systems and performance analysis of fading channels.

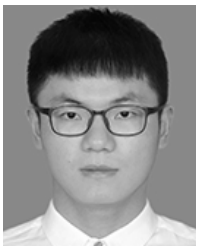

XU QIAO received the B.S. degree from the Nanjing Institute of Technology, Nanjing, China, in 2017. He is currently pursuing the M.S. degree with the College of Communication and Information Engineering, Nanjing University of Posts and Telecommunications (NJUPT), Nanjing. His research interests include wireless communications, massive MIMO, and mmWave hybrid precoding.

LONGXIANG YANG is with the College of Communications and Information Engineering, Nanjing University of Posts and Telecommunications (NJUPT), Nanjing, China, where he is currently a Full Professor and Doctoral Supervisor. His research interests span the broad areas of wireless networks, cooperative communications, and signal processing of communications. He has fulfilled multiple National Natural Science Foundations of China.